JOURNAL OF GEOPHYSICAL RESEARCH, VOL. 114, D00F16, doi:10.1029/2008JD011493, 2009

Organic aerosol formation in urban and industrial plumes near Houston and Dallas, Texas

R. Bahreini,[1,2] B. Ervens,[1,2] A. M. Middlebrook,[3] C. Warneke,[1,2] J. A. de Gouw,[1,2] P. F. DeCarlo,[4,5] J. L. Jimenez,[1,6] C. A. Brock,[3] J. A. Neuman,[1,2] T. B. Ryerson,[3] H. Stark,[1,2] E. Atlas,[7] J. Brioude,[1,2] A. Fried,[8] J. S. Holloway,[1,2] J. Peischl,[1,2] D. Richter,[8] J. Walega,[8] P. Weibring,[8] A. G. Wollny,[1,9] and F. C. Fehsenfeld[1,2]

Received 18 November 2008; revised 16 May 2009; accepted 4 June 2009; published 27 August 2009.

[1] We present measurements of organic aerosol (OA) in urban plumes from Houston and Dallas/Fort Worth as well as in industrial plumes in the Houston area during TexAQS-2006. Consistent with the TexAQS-2000 study, measurements show greater amount of aerosol mass downwind of the industrial centers compared to urban areas. This is likely due to higher emission and processing of volatile organic compounds (VOCs) from the industrial sources along the Houston ship channel. Comparisons of the current measurements with observations from the northeastern (NE) United States indicate that the observed ratios of the enhancement above background in OA, ΔOA, to the enhancement above background in CO, ΔCO, downwind of urban centers of Houston and Dallas/Fort Worth are within a factor of 2 of the same values in plumes from urban areas in the NE United States. In the ship channel plumes, $\Delta OA/\Delta CO$ exceeds that in the urban areas by factors ranging from 1.5 to 7. We use a chemical box model to simulate secondary organic aerosol (SOA) formation from anthropogenic and biogenic VOCs in different plumes using recently reported dependencies of SOA yields on VOC/NO_x ratios. Modeled SOA to CO enhancement ratios are within a factor of 2 of measurements. The increase in SOA from biogenic VOCs (BVOCs) predicted by the chemical box model as well as by a separate analysis using a Lagrangian particle dispersion model (FLEXPART) is <0.7 μg per standard m^3 (sm^{-3}). We find no evidence for a substantial influence of BVOCs on OA formation in our measurements in Houston area.

Citation: Bahreini, R., et al. (2009), Organic aerosol formation in urban and industrial plumes near Houston and Dallas, Texas, *J. Geophys. Res.*, *114*, D00F16, doi:10.1029/2008JD011493.

1. Introduction

[2] Aerosol particles in the Earth's atmosphere have gained much interest in recent years because of their negative effects on air quality, visibility and health, as well as effects on climate through their direct and indirect forcing. Sources of aerosol particles can be via direct (primary) emissions, as is the case for primary organic aerosols (POA), black carbon (soot), dust, and sea salt particles, or via secondary gas, surface, or particle phase reactions, as is the case for sulfate and secondary organic aerosol (SOA) species. In urban areas where a pool of gas-phase volatile organic compounds (VOCs) and inorganic precursors such as sulfur dioxide (SO_2) and nitrogen oxides (NO_x) exists, secondary formation and growth of aerosols are important sources, often dominating the total aerosol load. Several field studies in recent years have characterized the emissions, growth, and processing of aerosols in and downwind of polluted urban areas [*Brock et al.*, 2003; *Alfarra et al.*, 2004; *Drewnick et al.*, 2004; *Zhang et al.*, 2004; *de Gouw et al.*, 2005; *Volkamer et al.*, 2006, 2007; *Brock et al.*, 2008; *de Gouw et al.*, 2008; *DeCarlo et al.*, 2008].

[3] Although organic aerosols (OA) have been found to be abundant in the atmosphere and constitute a major fraction of submicron particles, both at the surface [*Zhang et al.*, 2007a] and in the free troposphere [*Heald et al.*, 2005; *Murphy et al.*, 2006], their formation and abundance

[1]Cooperative Institute for Research in Environmental Sciences, University of Colorado at Boulder, Boulder, Colorado, USA.
[2]Also at Earth System Research Laboratory, NOAA, Boulder, Colorado, USA.
[3]Earth System Research Laboratory, NOAA, Boulder, Colorado, USA.
[4]Department of Atmospheric and Oceanic Sciences, University of Colorado at Boulder, Boulder, Colorado, USA.
[5]Now at Paul Scherrer Institut, Villigen, Switzerland.
[6]Also at Department of Chemistry and Biochemistry, University of Colorado at Boulder, Boulder, Colorado, USA.
[7]Rosenstiel School of Marine and Atmospheric Science, University of Miami, Miami, Florida, USA.
[8]Earth Observing Laboratory, National Center for Atmospheric Research, Boulder, Colorado, USA.
[9]Now at Max Planck Institute for Chemistry, Mainz, Germany.

0148-0227/09/2008JD011493$09.00

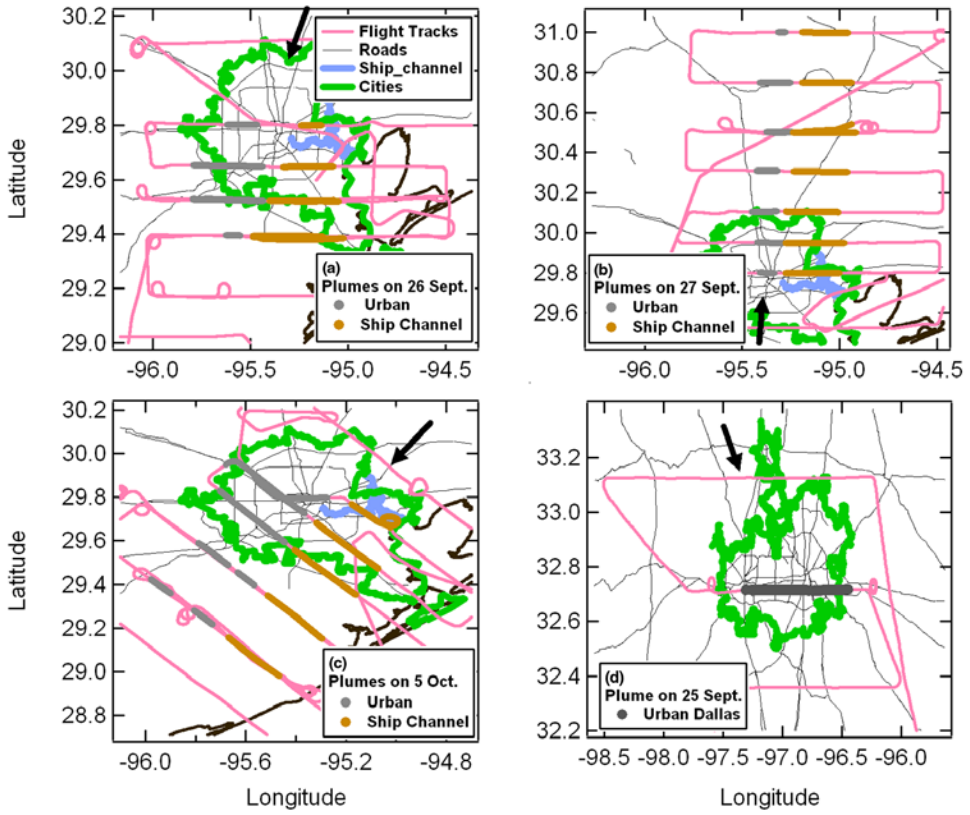

Figure 1. Flight tracks from flights on (a) 26 September, (b) 27 September, and (c) 5 October around Houston and (d) 25 September around Dallas/Fort Worth, Texas. Overlain on the flight tracks are the locations of Houston or Dallas/Fort Worth urban (gray points) and ship channel (mustard points) plumes on each day as identified in section 3.1. Arrows on each plot indicate the average wind direction for each measurement period.

is not yet well understood. In particular, the amount of SOA predicted in models using the measured concentrations of known precursor VOCs along with laboratory-based organic aerosol formation yields has been shown to be a factor of 3–100 lower than what is measured in the atmosphere [*de Gouw et al.*, 2005; *Heald et al.*, 2005; *Johnson et al.*, 2006; *Volkamer et al.*, 2006; *de Gouw et al.*, 2008; *Kleinman et al.*, 2008].

[4] Although both biogenic and anthropogenic sources contribute to SOA, their relative contribution differs considerably in many studies. Furthermore, with reductions in anthropogenic VOCs from urban and industrial areas [e.g., *Fiore et al.*, 1998; *Qin et al.*, 2007], it is of interest to compare the relative importance of anthropogenic and biogenic sources toward SOA formation. In an analysis of pollution from the NE United States, *de Gouw et al.* [2005] estimated 11% of OA to be POA, 68% to be SOA from anthropogenic sources, 12% to be SOA from biogenic sources while the remaining 9% of OA could not be attributed to any of these sources. Similarly, in urban plumes observed over the NE United States, no strong biogenic source for water-soluble organic carbon (WSOC) was identified [*Quinn et al.*, 2006; *Sullivan et al.*, 2006; *Weber et al.*, 2007]. However, radiocarbon analysis on WSOC collected on the ground in Atlanta, Georgia, and on filter-based OC samples in Nashville, Tennessee, and Tampa, Florida, indicated that ~50–90% of the measured particulate carbon was modern, i.e., originating from biogenic VOCs or from biomass burning [*Lewis et al.*, 2004; *Lewis and Stiles*, 2006; *Weber et al.*, 2007] rather than from fossil fuel sources. *Schichtel et al.* [2008] reported that modern carbon in Arizona and Washington comprised ~50% and ~80% of total carbon in the urban and near-urban areas, respectively. Radiocarbon analysis on summertime filter-based OC measurements at Aldine, Texas (a suburban site located ~27 km north of Houston), indicated that the fraction of modern carbon to total carbon varied between 25 and 68% whereas this fraction was 41–72% at Conroe, Texas (a forested site located ~65 km north of Houston) [*Lemire et al.*, 2002].

[5] In this study, we report on measurements of OA with a compact time-of-flight aerosol mass spectrometer [*Drewnick et al.*, 2005; *DeCarlo et al.*, 2006] and of primary and secondary VOCs by a proton transfer reaction mass spectrometer (PTR-MS) and by collection of air samples with a whole air sampler (WAS) and subsequent varied spectrometric analyses [*Schauffler et al.*, 2003; *de Gouw and Warneke*, 2007]. The measurements and samples were acquired aboard the NOAA WP-3D aircraft during the Texas Air Quality Study–2006 (TexAQS-2006). We compare the observed OA growth in urban and industrial plumes during TexAQS-2006 to that observed in previous studies. Using aerosol yields from recent laboratory studies, we interpret these measurements with the aid of a model of SOA formation. Improved agreement between predicted

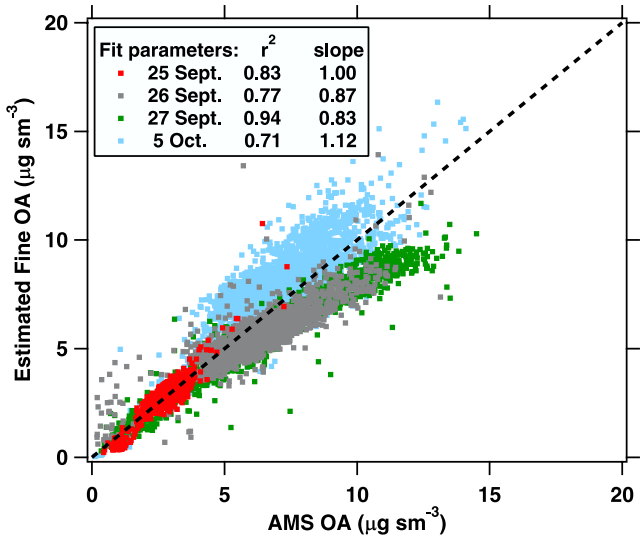

Figure 2. Comparison of AMS OA with OA estimated from fine volume measurements for the flights discussed here.

and observed OA growth relative to many previous comparisons shows the effect of these recently updated yields on predicted SOA formation. In addition, we use the Lagrangian particle dispersion model FLEXPART [*Stohl et al.*, 2005] along with a biogenic emission inventory (EPA BEIS3.12–3.13) and fixed SOA formation yields to estimate the amount of biogenic SOA formed from the predicted isoprene and monoterpenes in the sampled plumes.

2. Measurements

[6] An overview of the project, which included five instrumented aircraft, an instrumented ship, and ground supersites, is given elsewhere [e.g., *Parrish et al.*, 2009]. The NOAA WP-3D aircraft was based at Ellington Field, Houston, Texas, and performed 16 flights during 11 September to 12 October 2006. One of the main goals of the TexAQS-2006 study was to characterize urban and industrial emissions of various pollutants in the Dallas/Fort Worth, Texas, and Houston areas and to improve understanding of the transport and transformation of these pollutants. Therefore, most flight tracks of the WP-3D aircraft were designed to first sample background air upwind of the sources, and then sample the plumes immediately above and downwind of the Dallas/Fort Worth or Houston urban centers, industrial centers along the Houston ship channel, and Houston area power plants. Since the Houston ship channel, a heavily industrialized area along the shipping canal that extends from downtown Houston to Galveston Bay, is located mostly due east of the Houston urban center, we have selected data from 3 days when meteorology allowed for better separation of Houston's fresh urban and industrial plumes (Figures 1a–1c). For comparison with the Houston urban plume, we also present data from a flight over and downwind of Dallas/Fort Worth (Figure 1d). The Dallas/Fort Worth region is of comparable population and size to Houston, but does not have the intensive heavy industries associated with the Houston ship channel. Among the two WP-3D flights downwind of Dallas/Fort Worth, we present data from 25 September 2009 when chemical processing characteristics of the Dallas urban plume were similar to those in the Houston urban plume on 26 September. Although local biomass burning plumes were occasionally encountered during TexAQS [*Schwarz et al.*, 2008], on the basis of the observed mixing ratios of acetonitrile, a gas-phase species strongly associated with biomass combustion, the contribution of biomass burning to OA in the plumes discussed here is considered to be minimal.

[7] Aerosol composition aboard the aircraft was measured using a compact time-of-flight aerosol mass spectrometer (C-ToF-AMS, hereinafter "AMS," Aerodyne, Billerica, Massachusetts) through a low-turbulence inlet (LTI) [*Wilson et al.*, 2004], downstream of a 1 μm impactor [*Brock et al.*, 2008] and a pressure controlled inlet (PCI) [*Bahreini et al.*, 2008]. Details of the design and operation of the AMS are presented elsewhere [*Drewnick et al.*, 2005; *DeCarlo et al.*, 2006]. In short, aerosol particles are sampled through a critical orifice and a system of aerodynamic lenses where they are focused into a narrow beam. Non-refractory (NR) components of the particles are vaporized under high vacuum upon impaction on a tungsten inverted cone at ~550–600°C and ionized by electron impact. Ions are extracted into the detector region and analyzed using a compact time-of-flight mass spectrometer (Tofwerk, Thun, Switzerland). Mass-weighted size distributions are obtained by chopping the particle beam and measuring the time particles take to cross the vacuum chamber before detection in order to determine their vacuum aerodynamic diameter (d_{va}) [*DeCarlo et al.*, 2004]. Aerosol and gas-phase mass spectra are obtained by the difference between spectra acquired with a totally open and a totally blocked particle beam. Species concentrations at conditions of standard temperature and pressure (1 atm and 273 K, in μg sm^{-3}) are calculated from the mass spectra on the basis of the "fragmentation table" approach of *Allan et al.* [2004]. During TexAQS-2006 mass distributions and mass spectra were recorded every 10 or 15 s with a detection limit of 0.15 μg sm^{-3} for OA with a 10-s averaging time.

[8] The AMS collection efficiency (CE) was derived from the measured inorganic mass fraction and the sample relative humidity, using laboratory and other field CEs as a guide [*Quinn et al.*, 2006; *Matthew et al.*, 2008]. At times when small acidic sulfate particles were present, typically downwind of strong SO_2 sources, a size-dependent CE was applied. Aerosol size distribution measurements [*Brock et al.*, 2008], which were also made downstream of the 1 μm impactor, were used in combination with the AMS OA mass fraction and mass weighted density to estimate the amount of submicron OA mass (i.e., fine OA mass). Comparisons of AMS OA mass with the estimated fine OA mass show linear least squared correlation coefficients (r^2) of 0.71–0.94 (Figure 2). The flight-to-flight variation in the slopes of this comparison shows repeatability for AMS OA measurements to be better than ±25%. The overall uncertainty in the OA mass is estimated to be 38% (see auxiliary material for a comprehensive error analysis) and is consistent with other recent AMS aircraft studies [*DeCarlo et al.*, 2008; *Dunlea et al.*, 2008].[1] As described by *Bahreini et al.* [2008], using

[1] Auxiliary materials are available in the HTML. doi:10.1029/2008JD011493.

the PCI upstream of the AMS allowed for constant inlet pressure and flow rate into the instrument, fixed size calibration, and constant transmission (close to 100% in the size range of $d_{va} \sim 100-700$ nm, equivalent to physical diameters of $\sim$70–500 nm for particles with effective density of 1.4 g cm^{-3}), up to about 6.5 km in altitude. Transmission efficiencies for particles larger than d_{va} = 700 nm have not been fully characterized for this lens system; however, recent experiments in our laboratory on a similar lens system indicate that the transmission of larger particles decreases and approaches 50% for particles at $d_{va} \sim 900$ nm (equivalent physical diameter of 640 nm assuming an effective density of 1.4 g cm^{-3}). The closure between the AMS mass and fine mass to within the combined uncertainties however indicates that the effect of possible reduced transmission efficiencies for larger particles have been small in this data set.

[9] Measurements of gas-phase VOCs were made using a proton transfer reaction mass spectrometer (PTR-MS) [*de Gouw and Warneke*, 2007]. The PTR-MS scanned through a series of masses, with a cycle time of 16 s. In this study, we use the measurements of anthropogenic VOCs such as benzene, toluene, C8 and C9 aromatics and biogenic VOCs such as isoprene, the sum of its major oxidation products methyl vinyl ketone (MVK) and methacrolein (MACR), and the sum of monoterpenes. Some of the anthropogenic species, including anthropogenic isoprene, emitted from the petrochemical and rubber industries in the ship channel may also give rise to a PTR-MS signal at mass 69, which is usually attributed to biogenic isoprene; however, the contribution of these anthropogenic species to the total signal at mass 69 is estimated to be negligible in most ship channel air masses (C. Warneke et al., Biogenic emission measurements and inventories: Determination of biogenic emission in the Eastern United States and Texas and comparison with biogenic emission inventories, submitted to *Journal of Geophysical Research*, 2008). We also make use of the speciated VOC data from the whole air sampler, that collected air canisters in the plumes for offline GC-MS analysis [*Schauffler et al.*, 2003].

[10] Mixing ratios of CO (5% uncertainty) and SO_2 (10% uncertainty) were measured by vacuum UV resonance fluorescence and pulsed UV fluorescence, respectively, at 1 Hz [*Ryerson et al.*, 1998; *Holloway et al.*, 2000]. Mixing ratios of nitrogen oxides were measured at 1 Hz by ozone induced chemiluminescence for NO (5% uncertainty), by UV photolysis followed by NO chemiluminescence for NO_2 (9% uncertainty), and by catalytic reduction and subsequent NO chemiluminescence for NO_y (12% uncertainty) [*Ryerson et al.*, 1999, 2000]. Formaldehyde mixing ratios (13% uncertainty) were measured at 1 Hz using a tunable difference frequency generation gas absorption laser spectrometer (DFGAS) [*Weibring et al.*, 2007]. Data from an actinic flux spectroradiometer aboard the aircraft are used to calculate photolysis rates of various species as described by *Stark et al.* [2007]. In the current analysis, we use photolysis rates of O_3 (30% uncertainty for the channel to form $O^1(D)$), formaldehyde (15% uncertainty), and acetaldehyde (15% uncertainty) for OH calculations. For the analysis presented here, the above measurements were interpolated or averaged onto the AMS time base.

[11] In order to characterize the measurements in the Houston plumes analyzed for the current work, cumulative histograms of OA (Figure S7), SO_4^{2-} (Figure S8), NO_3^- (Figure S9), NH_4^+ (Figure S10), CO (Figure S11), benzene (Figure S12), SO_2 (Figure S13), NO (Figure S14), NO_2 (Figure S15), ambient relative humidity (Figure S16), ambient temperature (Figure S17), and calculated OH values (Figure S18) are provided in the auxiliary material.

3. Methodology for the Analysis

3.1. Plume Identification

[12] As described before, many aircraft flight patterns during TexAQS-2006 were designed to sample plumes downwind of downtown Dallas/Fort Worth or Houston, petrochemical and other heavy industries along the Houston ship channel, and in the power plants around Houston (Figures 1a–1d). In order to identify the sources of the plumes, mixing ratios of several primary gas phase species were considered. Many urban areas in the United States are characterized by [benzene]/[CO] $\sim$ 0.60–1.10 pptv ppbv^{-1} [*Warneke et al.*, 2007] due to automotive emissions, whereas this ratio can be much higher in some industrial plumes. For the analysis here, plumes with high SO_2 (>2–5 ppbv, depending on the day) or with [benzene]/[CO] > 2 pptv ppbv^{-1} were classified as "ship channel" plumes because of large sources of these compounds within the industrial area. In order to distinguish ship channel plumes from SO_2-rich plumes from power plants, the geographic location where the plumes were crossed relative to the power plants or the ship channel was also considered. Plumes with a predominant influence from the Houston urban center were classified by their higher-than-background CO (>120–180 ppbv, depending on the day), low benzene (<200–350 pptv, depending on the day), and low SO_2 (<2–5 ppbv, depending on the day) and are thus distinguished from plumes with ship channel and power plant influence. The urban plume downwind of Dallas/Fort Worth was identified by [benzene]/[CO] < 1 pptv ppbv^{-1} and CO > 120 ppbv. Moreover, in all the classifications, wind direction was considered in order to make sure plume assignments are consistent with the geographic distribution of the urban and industrial sources.

[13] Once different plumes were identified, background values of OA and CO for each plume in each transect were determined from measurements outside the plumes (values are given in Table S1 in Text S1 of the auxiliary material) and subtracted from the measured concentrations and mixing ratios. The enhancements in OA and CO above these background values are ΔOA and ΔCO, respectively. On 26 September and 5 October, when winds were from a northerly direction, OA and CO levels on the east side of the ship channel and west side of the urban plumes were similar in magnitude; therefore enhancements were based upon mean, background values calculated from $\sim$1 min of data each on the east side of the ship channel and the west side of the urban plumes. However, on 27 September, FLEXPART back trajectories indicate recirculation of the previous day's plumes over the western part of Houston. On this day, OA is $\sim$0.8–3 μg sm^{-3} higher and CO is $\sim$17–30 ppbv higher west of the urban plume compared with east of the ship channel, with the greatest longitudinal gradient being

observed on the second and third transects of the urban plume, ~40 km downwind of the city center. Background levels on this day are estimated on the basis of the values measured on the east side of the ship channel. This background gradient introduces the possibility of some bias in the calculated ΔOA and ΔCO, especially in the urban plume where background levels may be higher than for the ship channel plume on this day; we therefore provide an upper estimate of the bias in Figure S19 of the auxiliary material by calculating urban ΔOA and ΔCO values on the basis of background levels on the west of the urban plume. Background levels for the Dallas/Fort Worth flight (25 September) were determined from OA and CO measurements averaged for ~1 min each on the east and west of the urban plume downwind of the city. These determinations of ΔOA/ΔCO agree with OA to CO correlation slopes obtained from the linear orthogonal distance regression fits (see auxiliary material and Figures S20 and S21 therein).

3.2. Semiempirical Relations to Characterize OA Growth

[14] To compare OA production in plumes downwind of urban and industrial centers of Houston with those measurements made in the NE United States, we use the semiempirical relations of ΔOA/ΔCO that *de Gouw et al.* [2008] developed on the basis of observations in NE U.S. urban plumes. However, determining plume age requires additional consideration here. Since the emission ratios of toluene to benzene from the petrochemical industries in the ship channel are not the same for all sources and may vary in time, one cannot calculate the photochemical age on the basis of the ratio of toluene to benzene and their relative reactivity with respect to OH oxidation as defined by *de Gouw et al.* [2008]. Therefore, we calculate plume age from transport time rather than photochemical age. This transport age is determined from the perpendicular distance between the transect where the plumes were sampled and the center of Dallas/Fort Worth (at 32.760°N, 96.971°W), center of downtown Houston (at 29.759°N, 95.363°W), or center of the Houston ship channel (at 29.776°N, 95.102°W) and the averaged perpendicular component of the wind speed in the transect as measured aboard the aircraft. The wind speed measured on the aircraft during Houston flights is within 20% of the measurements by the wind profiler at La Porte, Texas, for the altitudes close to where the plumes were sampled. Uncertainty in the calculated transport age is estimated using 15 or 20 km uncertainty in the distance due to the dispersed nature of the sources for the ship channel and the urban areas, respectively, ±1 m/s uncertainty in the wind measurement, and the variability in the averaged wind speed in a transect. Note that although the absolute uncertainty in the calculated transport age is large, the uncertainty in our knowledge about the relative age is not; therefore, we believe it is valuable to explore the evolution of OA formation in different plumes on different days with respect to the transport age. Note that because of the different mixture and amounts of NO_x and VOCs in the ship channel compared to urban plumes, photochemical aging in the ship channel may be faster because of higher OH concentrations in the industrial plumes than in the urban plumes (Figure S18 in auxiliary material). Thus, transport age may represent different photochemical ages for plumes with different VOC and NO_x levels.

3.3. Box Model for Predicting OA Growth

[15] To calculate the formation of SOA downwind of urban and industrial plumes around Houston, we use a chemical box model in which several VOCs are allowed to oxidize and subsequently form SOA on the basis of the partitioning theory described by *Odum et al.* [1996]. This approach assumes that semivolatile species partition to particles by absorption (dissolution) into a liquid organic phase, and makes use of laboratory based SOA formation yields (Y) that can be expressed as

$$Y = M_0 \sum_{i=1}^{2} \left(\frac{\alpha_i K_{om,i}}{1 + M_0 K_{om,i}} \right) \quad (1)$$

where M_0 represents the preexisting organic aerosol mass onto which newly formed SOA material can be absorbed ("absorbing mass"), and α_i and $K_{om,i}$ are parameters for this two-product (i = 1, 2) model fitted to the yield observations ($Y = \Delta OA/\Delta VOC$) for a specific VOC precursor [*Odum et al.*, 1996]. The amount of absorbing mass has a crucial effect on the predicted SOA mass [e.g., *Ervens and Kreidenweis*, 2007]. In previous modeling studies the absorbing mass has been estimated as the sum of the primary organic aerosol (POA) mass, treated as the background, and the newly formed SOA mass [*Chung and Seinfeld*, 2002] although recent results suggest that hydrophobic POA may not provide a suitable partitioning medium for SOA [*Song et al.*, 2007]. Estimates of the fresh versus oxidized fraction of OA in the Texas plumes, determined from the organic mass spectral analysis of AMS data, indicate that less than 20% of OA is fresh and hydrocarbon-like (HOA) and more than 80% of OA is oxygenated OA (OOA) (see *Zhang et al.* [2005] for details on HOA and OOA analysis technique). This low fraction of HOA in the plumes is expected since the earliest transects occurred in the late morning, long after the nighttime boundary layer had dissipated, and thus primary combustion OA that is rich in HOA was mixed and diluted in the daytime boundary layer. In our base case simulations, we assume that the absorbing mass is equal to the sum of the background organic mass measured in each transect and the amount of SOA predicted in the box model in the previous transects. We explore the effect of partitioning only onto the OOA fraction of background organic aerosol in a sensitivity case where the absorbing mass is assumed to be the predicted SOA mass from the previous transects and 80% of the background organic mass.

[16] The box model is initialized with the measured mixing ratios of VOCs, NO_x, O_3, and the absorbing mass in the first transect of each plume, and it considers several VOC oxidation pathways outlined below. Using a pseudo–steady state approximation, OH concentrations along the flight tracks are calculated offline, averaged for each plume transect, and used in the model. This approximation considers OH formation through formaldehyde and ozone photolysis and OH loss through the reaction with NO_2 (see auxiliary material). The relative contribution from the formaldehyde photolysis channel to total OH concentration on 26 September and 5 October is determined and param-

eterized using the measured NO_2, acetaldehyde, and O_3 concentrations on these days. Unfortunately on 27 September, formaldehyde measurements were not available. However, since the measured ambient relative humidity (RH) on 27 September was within 15% of the average ambient RH on 27 September and 5 October, we use the average parameterization values as described above, along with OH concentration estimates from the O_3 photolysis channel on 27 September in order to estimate total OH concentrations on 27 September. Calculated OH concentrations for the days discussed here generally range from $\sim 2 \times 10^6$ to $\sim 2.5 \times 10^7$ cm^{-3}, depending on the plume and the day. These values are consistent with previous measurements and simulations for the TexAQS-2000 study at La Porte, Texas [*Mao et al.*, 2009; G. Frost, personal communication, 2008].

[17] By using the current literature parameters for equation (1) and the absorbing mass, certain amounts of semivolatile VOCs (SVOCs) from each precursor are predicted to form in each time interval between transects; these SVOCs are allowed to partition to the particle phase and form SOA. In each subsequent transect, the model is reinitialized using the mean of the calculated OH and the measured VOCs, NO_x, O_3, and the absorbing mass. Constrained by observations in this manner, the cumulative SOA mass produced throughout the plume history is calculated.

[18] We note that nontraditional anthropogenic SOA precursors, such as unmeasured VOCs with intermediate volatility or those involved in heterogeneous reactions, may also contribute to SOA formation [*Robinson et al.*, 2007; *Volkamer et al.*, 2007; *Shrivastava et al.*, 2008]; however, they are not considered in the current box model. Also, considering that the box model incorporates only the two-product parameterization rather than a full, chemical oxidation scheme, we are not able to carry through SVOCs from one transect to another, nor do we repartition SVOCs because of changes in the absorbing mass or gas phase partial pressure differences after dilution in the later transects. This means that VOC oxidation products are irreversibly partitioned to the particle phase in each transect. In addition, although SOA formation in aqueous phase and in clouds has previously been reported [*Sorooshian et al.*, 2006; *Carlton et al.*, 2007; *Sorooshian et al.*, 2007; *Ervens et al.*, 2008; *Hennigan et al.*, 2008; *Volkamer et al.*, 2009], the box model described here includes only gas phase oxidation of VOCs. On the days we examine, skies were clear to partly cloudy and ambient RH was mostly below 70%. Lack of an appreciable change in the measured SO_2 flux downwind of Parish power plant on the days discussed here indicate that cloud processing oxidation pathways have likely played at most a minor role [*Neuman et al.*, 2009].

3.3.1. Contribution From Anthropogenic VOCs

[19] Among the known anthropogenic SOA precursors, long-chain alkanes (i.e., C11 and higher) and aromatics have high measured SOA yields in the laboratory [*Seinfeld and Pandis*, 1998; *Lim and Ziemann*, 2005; *Ng et al.*, 2007b]. On the basis of WAS sample measurements of C4 to C8 alkanes, mixing ratios of alkanes decrease with increase in carbon number such that the sum of C7 and C8 alkanes is about a factor of two lower than their aromatic counterparts, toluene and C8 aromatics. If this trend continues for higher alkanes, we expect low concentrations of long-chain alkanes and minimal contribution to total SOA formation. With this in mind, because of lack of measurements of long-chain alkanes, we have only considered OH radical oxidation of benzene, toluene, and C8 and C9 aromatics, measured by the PTR-MS, as the formation process of anthropogenic SOA mass. Furthermore, since detailed yield information of only benzene, toluene, and xylene are available from laboratory experiments, we estimate the contribution of C8 and C9 aromatics to SOA formation as follows. Since WAS measurements indicated that xylene mixing ratios were higher than ethyl benzene by at least a factor of 2.5 [*Schauffler et al.*, 2003], we allow the sum of the C8 aromatics to be oxidized in the box model as xylene. However, with this assumption the amount of SOA from C8 aromatics is an upper limit. Speciated analysis of C9 aromatics by WAS samples indicate that the sum of the propyl benzene and ethyl toluene is on average a factor of 4–10 more abundant than trimethyl benzene. Since results from laboratory chamber studies indicate that SOA yields of propyl benzene and ethyl toluene are similar to that of toluene [*Odum et al.*, 1997], C9 aromatics are allowed to oxidize and form SOA with a yield equal to that of toluene.

3.3.2. Contribution From Biogenic VOCs

[20] Biogenic SOA was calculated using the measured mixing ratios of isoprene, MVK and MACR, and monoterpenes as proxies for biogenic SOA precursors. In the box model, we use $Y_{isoprene}$ along with the measured isoprene concentrations to estimate the amount of SOA formed from isoprene in each time step ($m(SOA)_{isoprene}$). In order to take into account isoprene oxidation that has taken place from the point of emission to sampling in the first transect ($t = t_1$), an additional isoprene "initial source," defined as $2 \cdot (MACR + MVK)_{t=t1}$, is calculated, considering that MACR and MVK are first generation oxidation products of isoprene with a combined yield of 50% [*Carter and Atkinson*, 1996]. Note that because MACR and MVK react with OH on the order of few hours themselves, it is possible that this calculation does not capture the full extent of isoprene oxidation. This additional "initial source" of isoprene is allowed to react away in the model throughout all time steps, i.e., without being reinitialized in each transect, and subsequently form SOA ($m(SOA)_{MACR+MVK}$):

$$m(SOA)_{MACR+MVK} = 2 \cdot [MACR + MVK]_{t=t_1} \cdot Y_{isoprene} \quad (2)$$

The total amount of SOA formed from isoprene can then be estimated as

$$m(SOA)_{isoprene,total} = m(SOA)_{MACR+MVK} + m(SOA)_{isoprene} \quad (3)$$

[21] To account for the contribution of different monoterpenes to SOA formation, on the basis of previous estimates of terpene emissions from different types of vegetation in the southeastern United States [*Geron et al.*, 2000], 2/3 of the measured monoterpenes were assumed to be α-pinene and 1/3 β-pinene. We used the two-product parameterizations for α- and β-pinene oxidation by OH and O_3 by *Griffin et al.* [1999] since both oxidation pathways can be important for SOA formation. Although oxidation of terpenes by the NO_3 radical can also be important [e.g., *Griffin et al.*, 1999], this oxidation scheme was not considered in our box model since only data from daytime flights

are presented. Given that monoterpene oxidation products were not measured, we cannot account for terpene oxidation that has taken place from the point of emission to sampling in the first transect ($t = t_1$) as we did for isoprene oxidation products; therefore, total contribution of monoterpenes to SOA formation may be underestimated in the box model.

[22] Sesquiterpenes were not measured in the present study. Furthermore, estimates for their emission ratios are highly uncertain and variable (~20–50% of monoterpenes) [*Ortega et al.*, 2007; *Sakulyanontvittaya et al.*, 2008]. Although recent laboratory studies have shown that selected sesquiterpenes (e.g., longifolene and aromadendrene) can form SOA with maximum yields that exceed those of monoterpenes by a factor of 2–4 (under comparable NO_x conditions) [*Ng et al.*, 2007a], we cannot estimate their contribution to total SOA because neither their concentrations nor mass- and NO_x-dependent yield parameters are available. However, in a sensitivity case discussed in section 5, we explore the possibility of SOA formation from sesquiterpene photooxidation, assuming sesquiterpene mixing ratios are 30% of the monoterpenes and have a constant SOA yield of 80%.

3.3.3. NO_x-Dependent SOA Yields

[23] Recent laboratory chamber studies have reported that SOA formation yields for various precursors are NO_x-dependent, which indicates a shift in the loss pathway of organo-peroxy radicals (RO_2) in the different NO_x regimes; under "high-NO_x" conditions RO_2 radicals tend to react preferentially with NO, forming alkoxy radicals and subsequently carbonyl compounds, whereas under "low-NO_x" conditions the reaction proceeds with HO_2, yielding organic hydroperoxides ROOH [*Kroll et al.*, 2005; *Presto et al.*, 2005; *Kroll et al.*, 2006; *Ng et al.*, 2007a, 2007b]. This shift in the chemistry affects volatility distribution of the oxidation products and thus the aerosol formation yields.

[24] In order to account for the NO_x dependence of SOA formation from aromatic VOCs and isoprene, we followed the same approach as used by *Henze et al.* [2008]. In this approach, the branching ratio of the loss reactions of RO_2 radicals due to the reaction with NO or HO_2 are calculated using the observed NO mixing ratios, which ranged from ~0.1–4 ppbv for the plume transects studied here, and an average HO_2 mixing ratio of 25 pptv (W. Brune, personal communication, 2008):

$$RO_2 + NO \rightarrow RO + NO_2$$
$$k^{1st}_{N,aromatics}(s^{-1}) = 8.5 \cdot 10^{-12}[NO] \quad \text{and}$$
$$k^{1st}_{N,isoprene}(s^{-1}) = 2.1 \cdot 10^{-12}[NO] \tag{4a}$$

$$RO_2 + HO_2 \rightarrow ROOH + O_2$$
$$k^{1st}_{H,aromatics}(s^{-1}) = 1.5 \cdot 10^{-11}[HO_2] \quad \text{and}$$
$$k^{1st}_{H,isoprene}(s^{-1}) = 7.45 \cdot 10^{-13}[HO_2] \tag{4b}$$

Using the branching ratio, the total yield for each VOC compound (aromatics or isoprene) is calculated by

$$Y_{VOC} = \frac{k_N^{1st}}{k_H^{1st} + k_N^{1st}} Y_{highNOx} + \frac{k_H^{1st}}{k_H^{1st} + k_N^{1st}} Y_{lowNOx} \tag{5}$$

along with the values for the mass-dependent $Y_{highNOx}$ and Y_{lowNOx} (equation (1)) by *Ng et al.* [2007b], *Kroll et al.* [2005, 2006], and *Henze and Seinfeld* [2006].

[25] The average HO_2 concentration of 25 pptv assumed in our calculations is an average value from daytime measurements in Houston in 2006 at the Moody Tower (about 80 m above ground) on the campus of University of Houston (W. Brune, personal communication, 2008); this value is also in the range of other measurements and simulations at La Porte, Texas, in 2000 [*Mao et al.*, 2009; G. Frost, personal communication, 2008]. However, previous measurements (and simulations) have indicated that although HO_2 levels are insensitive to NO mixing ratios for NO < 1 ppbv, the average value of HO_2 decreases by a factor of 3 when NO levels increase from 1 ppbv to 4 ppbv (the maximum value observed in Houston plumes discussed here). Although in the majority of the plumes, NO levels are <1 ppbv, we explore the effect of variable HO_2 mixing ratio in the NO-rich plumes in a case study further discussed in section 5.

[26] The yield parameters used to account for SOA formation from monoterpenes were determined at moderate NO_x/monoterpene ratios (about 1–4) [*Griffin et al.*, 1999] and do not take into account the NO_x dependence as observed for α-pinene by *Ng et al.* [2007a]. However, to date there is no α_i, K_i data set available for either compound that reflects the NO_x dependence. It has been shown that for α-pinene photooxidation, SOA yield can be a factor of 3 higher at low-NO_x conditions (NO_x/VOC < 1 ppbv ppbv^{-1}) than at high-NO_x conditions [*Ng et al.*, 2007a]. With the observed range of NO_x/monoterpenes >20 ppbv ppbv^{-1} in Houston, overall yields estimated from *Griffin et al.* [1999] are therefore upper limits; however, the error for total predicted SOA mass is small because of the small observed mixing ratios of monoterpenes as compared to the other precursors.

4. Observations and Discussion

4.1. Houston Urban and Industrial Plumes on 26 September and Dallas/Fort Worth Urban Plume on 25 September

[27] On 26 September, with northeasterly winds (at 3.6 ± 1.1 m s^{-1}), the WP-3D flew south–southwest of Houston (Figures 1a and 3a–3c), with 4–5 transects of downtown Houston and ship channel plumes within the well-mixed planetary boundary layer from 1230–1730 local time (LT) at an altitude of 300–450 m above sea level (Figure 4a). Nonrefractory composition of aerosols on this day, as on all others, was dominated by OA, with ammonium sulfate the second most prevalent compound (Figures S7–S10 in auxiliary material). Ship channel plumes were characterized by high benzene or SO_2 mixing ratios and urban plumes by enhanced CO (Figures 3a–3c and 4a). Enhanced SO_2 mixing ratios were also measured downwind of the Parish power plant, at 1425–1455 LT (Figures 3c and 4a). In Figure 5a, we present measurements of ΔOA/ΔCO versus transport age in the Houston urban and ship channel plumes on 26 September, averaged in each plume transect, with error bars representing standard deviations of the means. Higher values of ΔOA/ΔCO, by up to a factor of 7, were observed in the ship channel plume compared to the urban

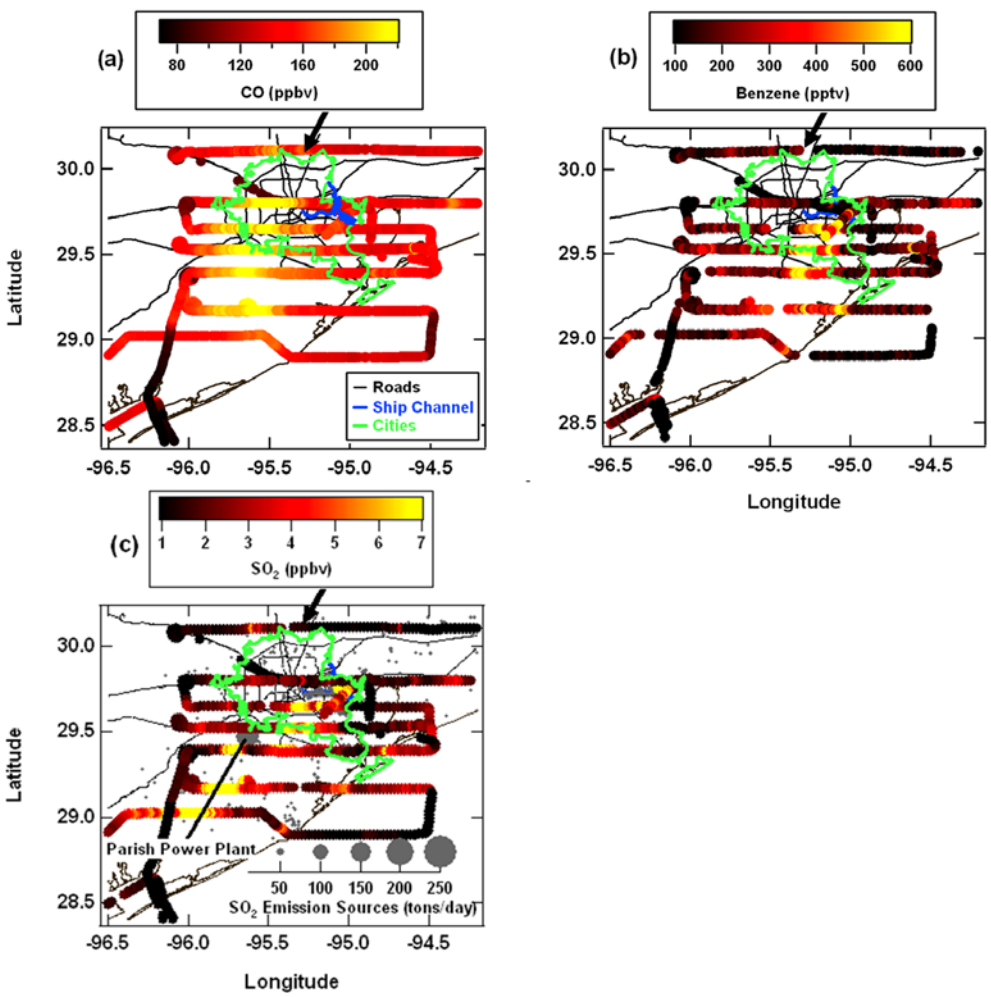

Figure 3. Flight track from 26 September, color coded with (a) CO, (b) benzene, and (c) SO_2. Point sources of SO_2 (gray points), sized with 2006 daily emission rates (G. Frost, personal communication, 2008), are indicated in Figure 3c. Arrows on each plot indicate the average wind direction.

plume. Values of ΔCO in the ship channel on 26 September were a factor of 2–4 lower than in the urban plume, and yet the amount of ΔOA in the ship channel was a factor of 2 higher than in the urban plume. Also shown in Figure 5a is the value of ΔOA/ΔCO in a transect downwind of Dallas/Fort Worth urban center sampled on 25 September (Figure 1d) and a semiempirical fit to data based upon observations from the NE United States [*de Gouw et al.*, 2008]. The solid line in Figure 5a represents an estimate of the primary emission of ΔOA/ΔCO, based on the measurements in early transects downwind of the Houston urban center on 26 September.

4.2. Houston Urban and Industrial Plumes on 27 September and 5 October

[28] Because of atmospheric circulation patterns in the Houston area, the diurnal changes due to the land-sea breeze circulation, and the geographical location of the urban and industrial centers that are only about 25 km apart, it is common for emissions from different sources in the area to mix, making it difficult to identify and sample isolated plumes with only urban or ship channel influence. This mixing is apparent in measurements of several gas phase species. For example, the ratio of benzene to CO is a factor of 6–12 higher in the ship channel plumes compared to urban plumes on 26 September whereas this ratio is only 2–5 on 27 September and 5 October (Figures 4a and 4b). Despite the mixing of the plumes on 27 September and 5 October, using the criteria outlined in section 3.1 we were able to identify plumes which were primarily influenced by fresh emissions from the ship channel or Houston urban areas (Figures 1b and 1c). In Figures 5b and 5c, we present measurements of ΔOA/ΔCO, averaged over each transect, as a function of transport age in plumes primarily associated with the urban and ship channel emissions on these days. Further discussion on the observed ΔOA/ΔCO patterns in these plumes is given in section 4.3.

4.3. Discussion on ΔOA/ΔCO Evolution in the Plumes

[29] In this section, we analyze the observations within plumes identified as being primarily of urban or industrial (ship channel) origin to look for differences in the growth of aerosol mass that can be attributed to differences in gas-phase precursor concentrations. Since CO is quasi-

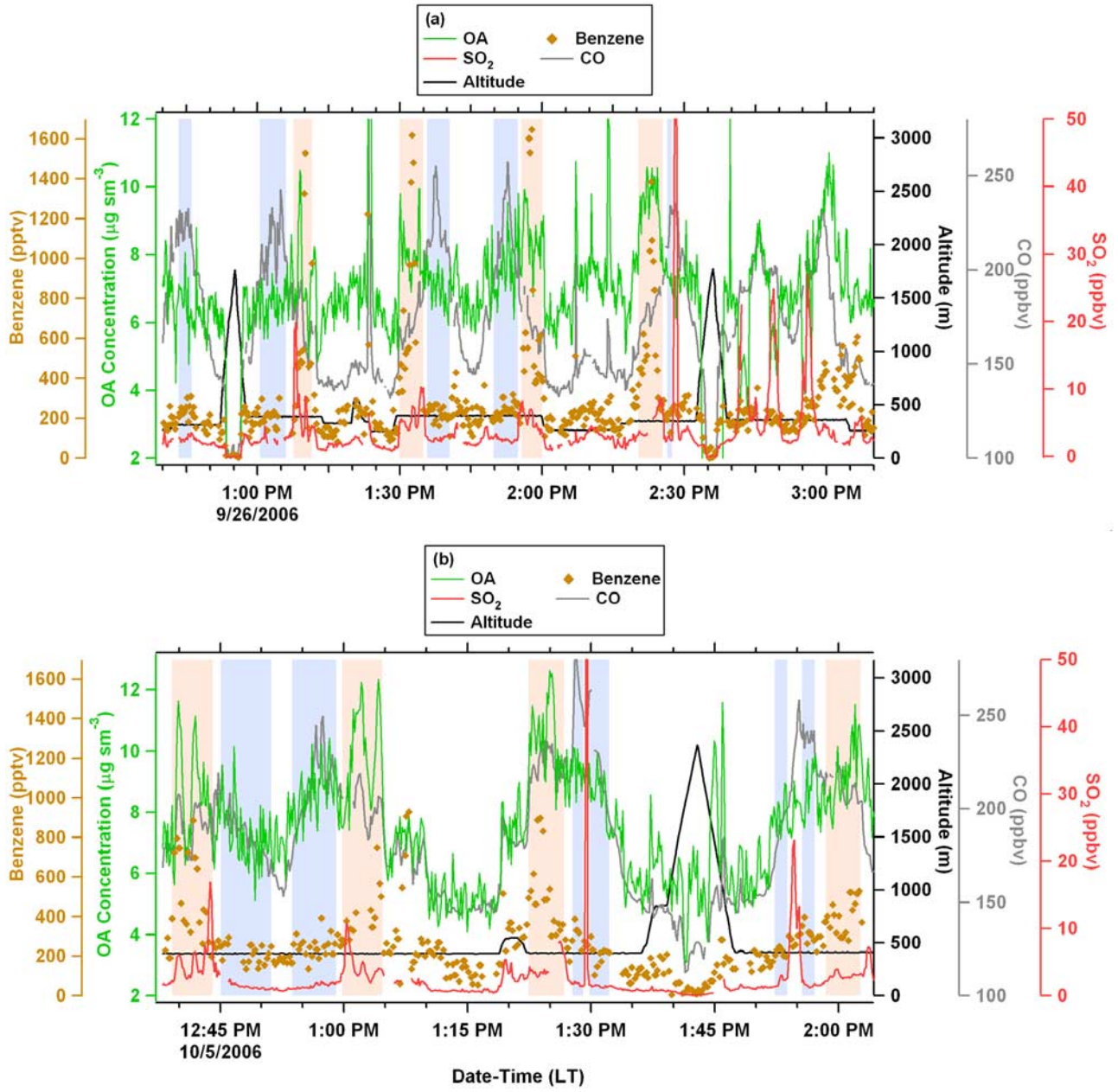

Figure 4. Time series of OA, benzene, CO, SO_2, and aircraft altitude in plumes transected south of Houston on (a) 26 September and (b) 5 October. Note that the peaks in SO_2 on 26 September from 1425 to 1455 LT and on 5 October from 1330 to 1355 LT indicate emission from the Parish power plant, sampled south of Houston (as indicated in Figure 3c for 26 September). Highlighted areas indicate urban (in light blue) and ship channel plumes (light red) as identified in section 3.1.

conserved over the time scales of our observations, and since it is emitted primarily by the transportation sector, we use it as a tracer to account for dilution of the emitted plumes with the surrounding air.

[30] The value of $\Delta OA/\Delta CO$ measured in the first transect downwind of the Houston urban center on 26 September was similar in magnitude to that in the first transect measured downwind of Dallas/Fort Worth on the previous day, suggesting that these large urban areas had similar precursor concentrations and chemical processes. Furthermore, for plume ages up to ~5 h, the Houston plume had $\Delta OA/\Delta CO$ values that were generally within a factor of 2 of similar measurements made downwind of urban plumes in NE United States [*de Gouw et al.*, 2008]. Note that because of the close proximity of the sampling region to downtown Houston and the ship channel, relatively fresher plumes were sampled in TexAQS compared to those sampled downwind of urban centers in the NE United States. Despite scatter in the data and large uncertainties in the derived values of $\Delta OA/\Delta CO$, it is evident that the increase in $\Delta OA/\Delta CO$ with age was substantially greater in the

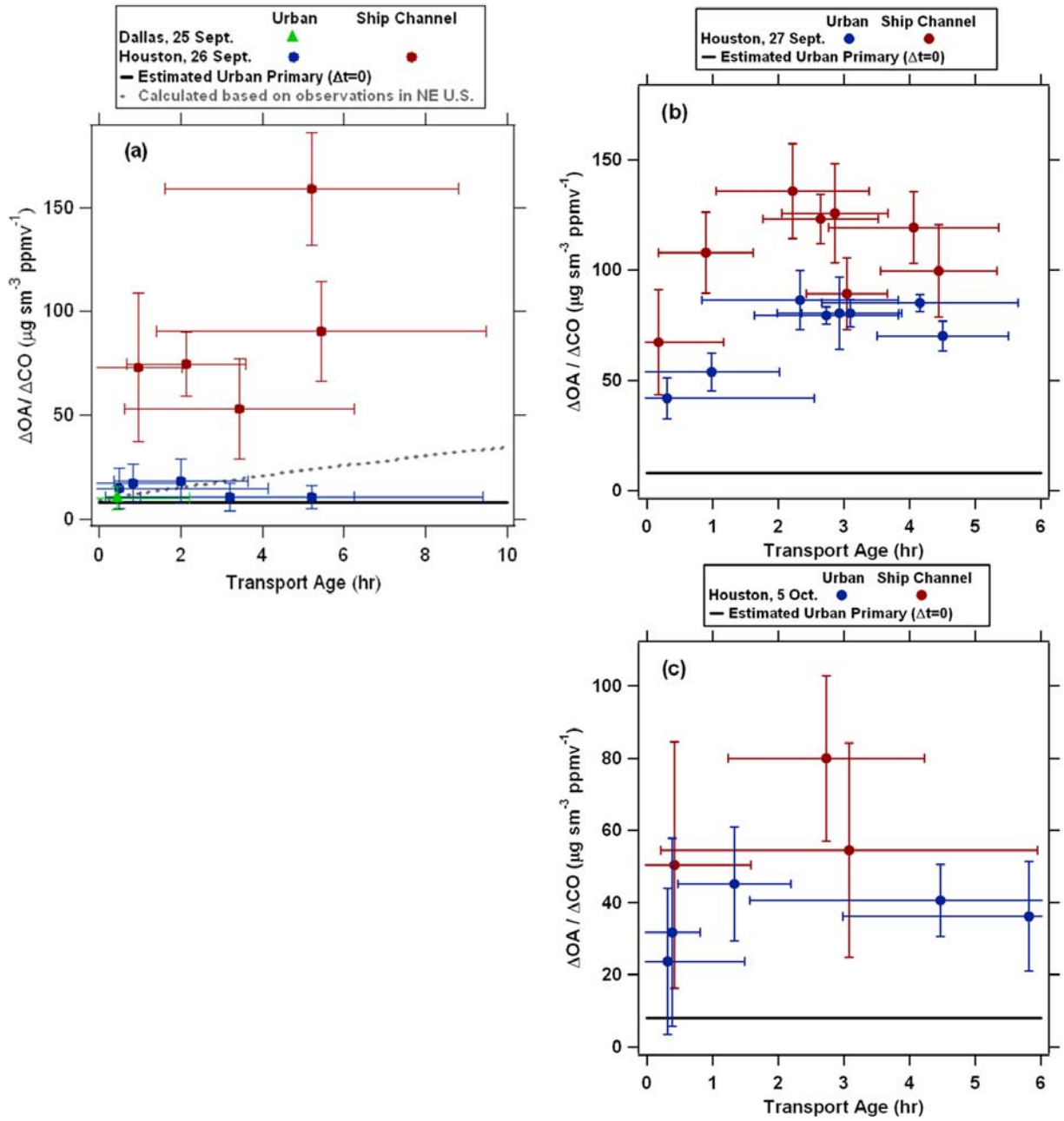

Figure 5. Evolution of ΔOA/ΔCO with transport age from (a) Dallas urban plume on 25 September and Houston urban and ship channel plumes on 26 September, (b) Houston urban and ship channel plumes on 27 September, and (c) Houston urban and ship channel plumes 5 October. Error bars for ΔOA/ΔCO indicate standard deviation from the mean in each transect. Error bars in transport age indicate the uncertainty in the estimated age. The dashed line in Figure 5a represents calculations of ΔOA/ΔCO based on observations in NE United States [*de Gouw et al.*, 2008]. The solid lines represents estimated urban primary ΔOA/ΔCO based on observations in Texas.

ship channel plumes than in those from the urban areas (Figure 5a).

[31] While values of ΔOA/ΔCO observed in urban plumes in Houston (26 September) and Dallas/Fort Worth (25 September) were within a factor of 2 of those measured in the NE United States, the increases observed in the VOC-rich ship channel plume on 26 September were greater by a factor of ~1.5–7 (Figure 5a). Note that because of higher concentrations of OH in the ship channel plumes (Figure S18 in auxiliary material), photochemical aging in these plumes is expected to be faster than in the urban plumes. Among the urban VOCs measured in the atmosphere, aromatics are among the compounds with the highest measured SOA-forming potential [*Seinfeld and Pandis*, 1998]. The sum of the measured aromatics relative to CO as a function of plume age on 26 September is shown in Figure 6. Considering that the initial carbon mixing ratios of aromatics in the urban plumes were approximately a

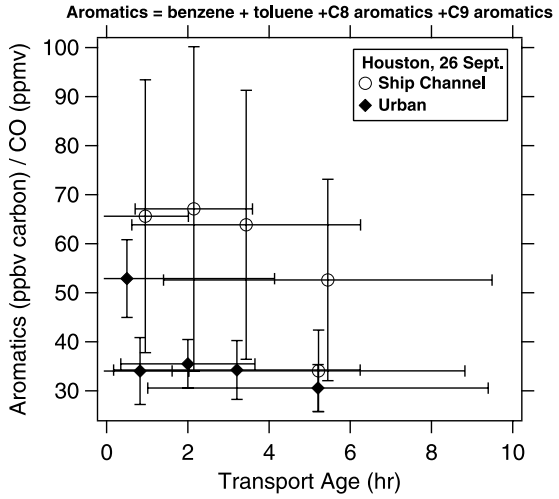

Figure 6. Comparison of the ratio of measured mixing ratios of aromatics (ppbv of carbon) to CO (ppmv) in the ship channel and urban plumes on 26 September and their decay with transport age. Error bars indicate standard deviation from the mean in each transect.

factor of 2 lower than those in the ship channel, the ship channel plumes had at least twice the potential for SOA formation from these precursors under similar NO_x conditions. Additionally, the factor by which the ratio of aromatics to CO decreased over time downwind of the ship channel (Figure 6) is similar to the factor by which ΔOA/ΔCO in the ship channel increased on 26 September (Figure 5a) over a similar period of time.

[32] Despite this clear evidence for enhanced production of OA relative to CO in the plumes from the ship channel industries relative to those from the urban centers, there is much scatter and variability in the data. Values of ΔOA/ΔCO observed on 27 September and 5 October were significantly higher than the estimated primary ratio of ΔOA/ΔCO from 26 September, demonstrating the large contribution from SOA. As indicated in Figure 7, the box model also predicts higher values of ΔOA/ΔCO in the urban-influenced plumes on 27 September and 5 October compared to 26 September, indicating greater contribution from primary VOCs to SOA formation in these polluted urban-influenced plumes. However, the differences between measured ΔOA/ΔCO values in the ship channel– and Houston-influenced plumes on these days were not as large as in the plumes on 26 September. Decay in the ratio of aromatics to CO in the ship channel–influenced plumes with transport age was faster on 27 September and similar on 5 October compared to 26 September. This further indicates that some secondary production of OA occurred in these plumes; however, continuous and appreciable increase in ΔOA/ΔCO with age on 27 September and 5 October is not obvious.

[33] With dilution of the plumes downwind of the sources, it is possible that SVOC components of the aerosol repartitioned back to the gas phase because of a reduction in their gas phase partial pressure [*Grieshop et al.*, 2007]. Although the extent to which this occurred is not known, it is plausible that because of this repartitioning, the ΔOA/ΔCO may not have increased as a function of plume age as rapidly on days when mixing and dilution were stronger (for example on 27 September when observed wind speed was 4–10 m/s). Additionally, point and area sources of VOCs and CO away from the urban center and the ship channel may have also contributed to the measured OA and CO as the plumes aged. Mixing of these fresher emissions with plumes originating from the Houston urban center and the ship channel may have contributed to the observed scatter in ΔOA/ΔCO, since plume ages were determined from transport time from the center of the urban or ship channel. Moreover, because of the mixing of urban- and ship channel–influenced plumes on 27 September and 5 October with aged, recirculated urban/industrial plumes, evolution of ΔOA/ΔCO on these days was more difficult to evaluate than on 26 September. This also implies that the values of ΔOA/ΔCO on 27 September and 5 October may not have been typical for plumes emitted into a relatively clean background.

[34] Finally, an increase in ΔCO due to secondary formation of CO might have caused a reduction in the observed ΔOA/ΔCO. Previous modeling studies have shown that anthropogenic contribution to CO concentrations in Los Angeles and in the New England area is dominated by primary sources, with secondary production of CO from anthropogenic VOCs contributing <1% in Los Angeles [*Griffin et al.*, 2007] and 10–30% in New England [*Griffin et al.*, 2007; *Hudman et al.*, 2008]. We have calculated the instantaneous production rate of CO from the measured concentrations of formaldehyde and acetaldehyde in ship channel and urban plumes. Average production rates are ~1.1 ppbv CO/h and ~2.3 ppbv CO/h in the urban and ship channel plumes, respectively. These production rates result in ~6.6 ppbv and ~14 ppbv of CO produced in the urban and ship channel plumes, respectively, after 6 h of transport. Since at Δt = 6 h of transport age, ΔCO in the urban plumes is ~30–80 ppbv and in the ship channel

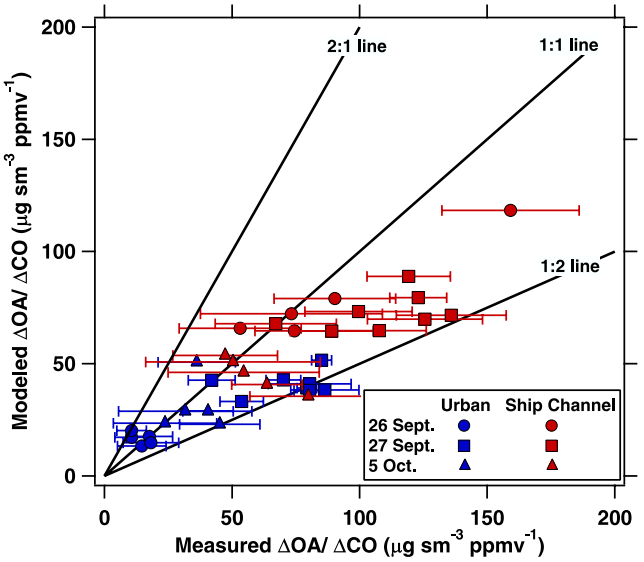

Figure 7. Comparison of the box model results with measurements as the scatterplot of ($SOA_{modeled}$ + $\Delta OA_{measured,\ first\ transect}$)/$\Delta CO_{measured}$ (i.e., modeled ΔOA/ΔCO) versus the measured values of ΔOA/ΔCO.

Table 1. Results of the Box Model to Estimate the Fractional Contribution of Individual VOCs, Sum of Biogenic VOCs, and Sum of Anthropogenic VOCs to the Modeled SOA in Urban and Ship Channel Plumes at the End of the Simulation[a]

Fractional Contribution to SOA	26 September		27 September		5 October	
	Urb	SC	Urb	SC	Urb	SC
$f_{isoprene}$	0.16	0.15	0.27	0.27	0.11	0.09
$f_{MVK+MACR}$	0.37	0.16	0.22	0.17	0.33	0.16
$f_{monoterpene}$	0.02	0.02	0.02	0.03	0.03	0.02
$f_{benzene}$	0.03	0.11	0.05	0.09	0.06	0.11
$f_{toluene}$	0.18	0.26	0.22	0.21	0.24	0.3
$f_{C8\text{-}aromatics}$	0.19	0.23	0.19	0.19	0.16	0.25
$f_{C9\text{-}aromatics}$	0.05	0.07	0.03	0.04	0.07	0.07
$f_{biogenic}$	0.55	0.33	0.51	0.47	0.47	0.27
$f_{anthropogenic}$	0.45	0.67	0.49	0.53	0.53	0.73

[a]Urb, urban; SC, ship channel. Depending on the day and the plume, $\Delta t \sim 3-6$ h. Note that $f_{isoprene}$ is the term accounting for oxidation of isoprene measured in the plumes while $f_{MVK+MACR}$ is the term accounting for oxidation of additional "initial isoprene source" as explained in section 3.3.2.

plumes ~20–60 ppbv, the CO produced through secondary oxidation may have contributed ~8–18% of the ΔCO in the urban plumes and ~25–70% in the ship channel plumes. Hence, accounting for secondary production of CO could cause ΔOA/ΔCO to increase by a factor of ~1.1–1.2 and ~1.3–1.8, in the urban and ship channel plumes (at $\Delta t = 6$ h), respectively.

[35] We conclude that the combination of all the factors discussed above, namely, repartitioning of SVOCs to the gas phase after dilution, contribution from other sources located downwind of the urban center and the ship channel, mixing with recirculated pollution, and secondary production of CO in the plumes may have reduced the values of ΔOA/ΔCO at longer transport ages on 27 September and 5 October compared with other days which showed larger SOA production.

5. Comparison With Box Model Results

[36] To compare the predicted amount of SOA with observations, we have calculated $(SOA_{modeled} + \Delta OA_{measured,\ first\ transect})/\Delta CO_{measured}$ in each transect. These results are compared with the measured values of ΔOA/ΔCO in Figure 7. The reason for adding the measured ΔOA in the first transect to the modeled SOA values is to account for ΔOA that was already present in the first transect since SOA formation in the box model starts from zero in this transect.

[37] Contributions of individual VOCs to the total SOA predicted by the box model are summarized in Table 1. Among anthropogenic VOCs, toluene and C8 aromatics dominate the SOA fraction, each contributing ~20% on average. Partitioning from oxidation of the C9 aromatics contribute <7% to the predicted total SOA. Modeled SOA from isoprene and its oxidation products dominate the biogenic SOA. The modeled biogenic fraction of SOA is dominant (i.e., >50%) over the modeled anthropogenic fraction in the urban plumes on 26 September and 5 October; however, the modeled anthropogenic fraction is always dominant (i.e., >50%) in the anthropogenic VOC (AVOC)-rich ship channel plumes.

[38] Previous modeling studies underestimated SOA mass by a factor of 8–30 for air masses with a photochemical age of 1–10 h [*Volkamer et al.*, 2006]. However, as shown in Figure 7, our modeled ΔOA/ΔCO values are within a factor of 2 of the average values measured in the cases described above. The following differences between our box model and other SOA prediction models have improved the agreement between observed and predicted SOA mass:

[39] 1. In our model, we have included benzene as an SOA precursor. Additionally, in some of the previous studies, constant SOA yields of 10% for both toluene and xylene, obtained under high-NO_x and high amounts of absorbing mass [e.g., *Seinfeld and Pandis*, 1998], have been applied to estimate SOA formation. Mass- and NO_x-dependent yields from more recent laboratory studies are used in our analysis and result in yields of 12–21% for benzene, 7–15% for toluene, and 5–14% for xylene, for the conditions encountered in TexAQS. This leads to an overall increase in the total predicted anthropogenic SOA mass by up to a factor of ~1.3, compared to using an assumed 10% SOA yield for toluene and xylene only.

[40] 2. We have also considered SOA formation through secondary oxidation of MACR and MVK to account for oxidation of isoprene prior to the first transect. The amount of SOA from this pathway is on average 25% of the total SOA (Table 1), resulting in an increase in total SOA by a factor of ~1.3 compared to a case where this pathway is not considered.

[41] 3. In most of the previous studies, only aerosol yields from high-NO_x conditions have been applied to the models, whereas under reduced NO_x conditions SOA formation from aromatics, isoprene, and monoterpenes may occur at significantly higher yields [*Presto et al.*, 2005; *Kroll et al.*, 2006; *Ng et al.*, 2007a, 2007b]. Assuming a mixing ratio of 25 pptv for HO_2, the model results indicate that at least 0.05 ppbv of NO is needed in order to have more than 50% of the aromatics following the high-NO_x reaction scheme; this corresponds to total of 0.3 ppbv of NO_x in the plumes studied here. Since NO_x mixing ratios decrease with plume age for most plumes studied here, the fraction of aromatics that reacted through the high-NO_x oxidation pathway (equation (4a)) decreased from ~100% at the first transect to ~65–90% at $\Delta t = 6$ h, depending on the day. For isoprene-RO_2 radicals that have a much lower rate constant with HO_2, at least 0.01 ppbv of NO is needed to have more than 50% of isoprene react through the high-NO_x pathway. Thus, in the transects farthest downwind of the sources, the high-NO_x (i.e., lower SOA yield) isoprene oxidation pathway contributed >90% of isoprene oxidation. In summary, our model results show that the low-NO_x pathway contributed to 10–35% and 10% of the oxidation of aromatics and isoprene, respectively. Considering the differences in the yield values in the low- and high-NO_x regimes, an additional 10–55% and 2–15% of SOA from aromatics and isoprene, respectively, were formed from the low-NO_x pathway. For the conditions encountered during TexAQS-2006, the amount of predicted SOA is increased by up to a factor of 1.7 by considering the low-NO_x pathway. This trend is consistent with study of *de Gouw et al.* [2008] who

reported that using only the low-NO_x SOA yields of aromatics to obtain an upper limit of SOA production reduced the discrepancy between measured and predicted SOA production from a factor of 10 to ~3 in the NE United States.

[42] Combining the enhancement factors listed above indicates that by considering SOA formation from benzene and MACR-MVK as well as considering the absorbing mass- and NO_x-dependent SOA yields, about a factor of 3 improvement in the agreement between modeled and measured SOA values is achieved.

[43] As discussed in section 3.3, we have run a sensitivity test with only the OOA fraction (80%) of the background organics and the newly formed SOA as the absorbing mass. Results indicate that with a 20% reduction in the amount of background absorbing mass due to the presence of HOA, modeled amounts of SOA is reduced by about 5%. Sensitivity runs with reduced mixing ratio of HO_2 in the plumes where NO > 1 ppbv result in reduction of total SOA by <2%.

[44] We also explored the role of sesquiterpenes in biogenic SOA formation, where sesquiterpenes were estimated to be 30% of the monoterpenes, representative of the average estimated emission ratio of sesquiterpenes to monoterpenes [*Sakulyanontvittaya et al.*, 2008]. Since most of the biogenic VOCs (BVOCs) are emitted outside the urban and industrial areas of Houston, and since sesquiterpenes have higher reactivity with OH and O_3 compared to monoterpenes, this leads to overestimating the mixing ratios of sesquiterpenes in the plumes. With this in mind, if sesquiterpenes are allowed to form SOA with a yield of 80%, the amount of biogenic SOA would increase by up to a factor of 2.7.

[45] To summarize, as indicated in Figure 7, the box model shows improved agreement between modeled and measured values of $\Delta OA/\Delta CO$ when accounting for the currently known SOA formation schemes. However, uncertainties remain in the identity of both anthropogenic and biogenic SOA precursors and nontraditional SOA formation processes that lead to underestimating SOA formation in the box model by up to a factor of 2. Because of these caveats, we cannot use the modeled fractions of biogenic versus anthropogenic OA conclusively. We rather explore the role of BVOCs and AVOCs in SOA formation in section 6, using our measurements of OA and anthropogenic pollution tracers that show no evidence for significant additional OA formation from BVOCs in plumes with high anthropogenic influence.

6. Role of BVOCs in SOA Formation

[46] In addition to the box model calculations of SOA from BVOCs described in sections 3.3 and 5, we used a Lagrangian particle dispersion model to estimate mixing ratios of BVOCs along the flight track. For this analysis, we added the EPA BEIS (BEIS 3.12–3.13) [*Pierce and Waldruff*, 1991; *Pierce et al.*, 1998] emission inventory for isoprene and monoterpenes to the Lagrangian particle dispersion model, FLEXPART [*Stohl et al.*, 2005]. As described by Warneke et al. (submitted manuscript, 2008), the mixing ratios of isoprene calculated using FLEXPART's 1-h footprint were within a factor of 2 of the isoprene measured aboard the aircraft. In a similar comparison for monoterpenes, FLEXPART's estimate was at times a factor of 2 higher than the measurements and thus may lead to an overestimation of biogenic SOA formation; however, this is still within the uncertainties of monoterpene emissions and measurements (Warneke et al., submitted manuscript, 2008). For our analysis here, we allow the amount of isoprene and monoterpenes, predicted to be present in the plumes by FLEXPART's 72-h footprint, to oxidize and form SOA using constant SOA formation yields. SOA yields assumed here (2.5% for isoprene and 10% for monoterpenes) are the averaged overall yields calculated in the box model that correspond to the NO_x/VOC ratios and absorbing mass estimates during the flights. However, some oxidation of isoprene and monoterpenes might have occurred with different SOA yields in earlier parts of the transport when the NO_x/VOC ratios or the absorbing mass were different. The amount of SOA (in $\mu g\ sm^{-3}$) formed from the BVOCs is calculated by multiplying the above yields and the corresponding concentration of BVOCs in $\mu g\ sm^{-3}$. Note that this analysis does not allow for reversible partitioning of BVOC oxidation products, and therefore represents an upper estimate of the SOA formed.

[47] Figure 8 shows the enhancement in OA (ΔOA) that is predicted from BVOCs in the box model as well as the amount that is predicted by oxidation of isoprene and monoterpenes in FLEXPART as a function of transport age for plumes transected on 27 September, when plumes with higher influence of biogenic emissions were sampled north of Houston. Since SOA formation in the box model is initialized with zero SOA in the first transect, for this comparison, the background value of 0.37 $\mu g\ sm^{-3}$ estimated from FLEXPART in the initial transects (i.e., transport age ~ 0 h) has been subtracted from total OA values predicted by FLEXPART. The two methods agree well in predicting the time scale of increase in OA. In addition, the enhancement in biogenic OA predicted from either method is <0.7 $\mu g\ sm^{-3}$ and the two methods differ by <34% for predicting the enhancement due to biogenic OA. As mentioned in section 3.3, the box model accounts for earlier oxidation of isoprene in an air mass by adding $2 \cdot (MACR + MVK)_{t=t1}$ in the isoprene budget (equations (2) and (3)) whereas FLEXPART directly accounts for total isoprene footprint in the past 72 h. The good agreement in predicted total biogenic OA by the two methods indicates that the box model is reasonably accounting for the oxidation of total isoprene.

[48] Although the model comparisons of $\Delta OA/\Delta CO$ with measurements are in better agreement than in previous studies, there is still up to a factor of 2 discrepancy when average modeled $\Delta OA/\Delta CO$ values are compared with the average measured values in each transect (Figure 7). As mentioned in sections 3.3 and 5, our understanding of both the biogenic and anthropogenic SOA precursors, in terms of their identity, ambient precursor concentration, SOA yield, and gas to particle partitioning, is incomplete. Therefore, it is necessary to consider the relationship between anthropogenic and biogenic organic aerosol precursors in order to identify the dominant processes responsible for OA formation in the region.

[49] In Figure 9a, we present the scatterplot of OA versus CO on 27 September. A positive correlation of OA versus

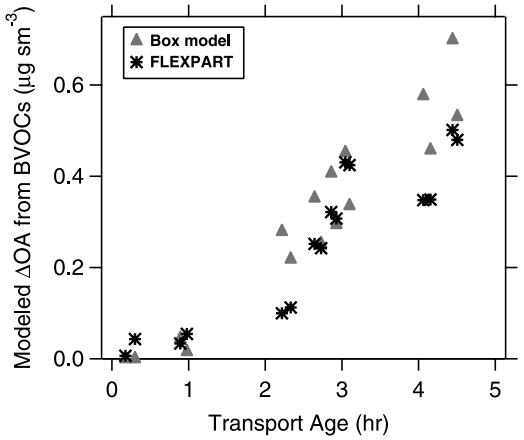

Figure 8. Evolution of enhancement in OA from BVOCs predicted by the box model and from analysis of FLEXPART with the 72-h isoprene and monoterpene surface contribution input with transport age for plumes transected on 27 September. Estimated background value of 0.37 μg sm^{-3} has been subtracted from FLEXPART predicted OA values.

CO is observed, with a slope of 92 μg sm^{-3} ppmv^{-1} and r^2 = 0.87. This slope does not change significantly if only data points over the forested site north of Houston with [BVOC] > 1500 pptv are considered. Although secondary CO production through oxidation of BVOCs is also possible, a correlation of r^2 = 0.64 between acetylene, an anthropogenic marker, and CO (Figure 9b) indicates that sources of CO in Houston area are mainly anthropogenic. (The outliers in this scatterplot show enhancements in benzene, indicating the different emission ratios of acetylene to CO in different industries of the ship channel.) Therefore, the strong correlation of OA with CO and insensitivity of the OA/CO slope to biogenic sources strongly suggests that in the time scale of few hours when anthropogenic precursors are transported to areas with a strong biogenic influence, there is no evidence in our measurements for significant additional OA production from BVOCs. This finding is consistent with previous observations in the NE United States [*Sullivan et al.*, 2006; *Weber et al.*, 2007; *de Gouw et al.*, 2008] that indicate a strong link between anthropogenic emissions and SOA formation.

7. Comparison to Measurements From the TexAQS-2000 Study

[50] The OA growth shown here helps explain the aerosol growth observed in a previous study in the same region. During the first Texas Air Quality Study in 2000 (TexAQS-2000), measurements of particle size distributions, NO_x, SO_2, and VOCs were made aboard the NCAR Electra aircraft, downwind of urban and industrial centers around Houston [*Brock et al.*, 2003]. Particle volume measurements downwind of an isolated, rural power plant, which was a strong source of SO_2, showed that the observed growth was consistent with gas phase SO_2 oxidation and the subsequent gas to particle condensation and neutralization of H_2SO_4. However, downwind of the ship channel industries, the growth in particle volume exceeded the amounts predicted from gas to particle partitioning of SO_2 oxidation products by factors of 2–10. Although particle composition measurements were not available aboard the Electra aircraft in 2000, it was speculated at the time that the unaccounted increase in particle volume was due to nitrate and/or SOA formation [*Brock et al.*, 2003].

[51] In Figure 10, we compare the volume-based aerosol growth measurements on 26 September 2006 with the measured growth on 27–28 August 2000 presented by *Brock et al.* [2003]. The average volume-based aerosol data from TexAQS-2000 were about a factor of 2–5 higher than the average volume-based aerosol measurements during TexAQS-2006. Comparing the modeled values of the ratio of particulate sulfur to total sulfur (SO_4^{2-}/(SO_4^{2-} + SO_2 (g)))

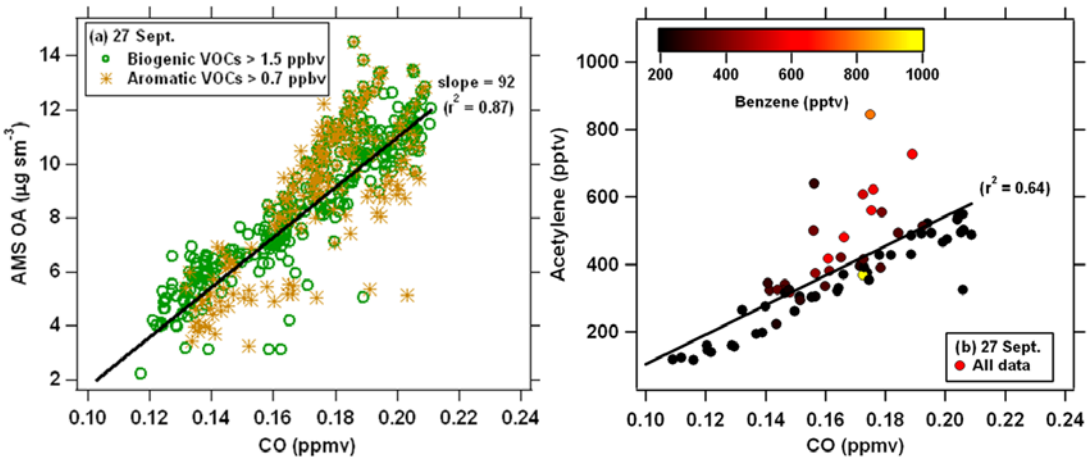

Figure 9. (a) Scatterplot and linear fit of OA versus CO on 27 September. Data points from plumes with higher influence of biogenic (i.e., isoprene + 2 (MVK + MACR) + monoterpenes) and aromatic (i.e., sum of C6-C9 aromatics) VOCs are shown in green and brown, respectively. (b) Scatterplot and linear fit of acetylene versus CO for all the data points from 27 September. The markers are colored with mixing ratio of benzene.

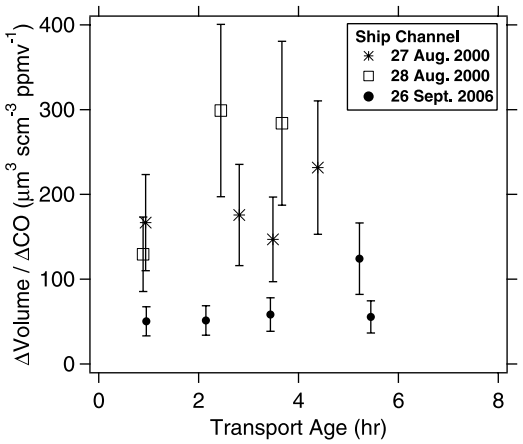

Figure 10. Comparison of aerosol growth, presented as ΔVolume/ΔCO (μm^3 scm^{-3} $ppmv^{-1}$), in ship channel plumes during TexAQS-2000 [*Brock et al.*, 2003] and TexAQS-2006 studies. Error bars indicate the uncertainty (34%) in the volume measurements.

in 2000 and the values measured in 2006 indicate that the degree of oxidation in the plumes from 27 to 28 August 2000 and 26 September 2006 was similar. However, VOC measurements in 2006 indicate that the median mixing ratio of many VOCs, including aromatics that are among the dominant known SOA precursors, were a factor of 2 lower in 2006 compared to 2000 (E. B. Cowling et al., The final rapid science synthesis report: Findings from the Second Texas Air Quality Study (TexAQS II), available at http://www.esrl.noaa.gov/csd/2006/rss/rsstfinalreport083107.pdf). Moreover, in 2006 temperatures were lower, wind speeds higher, and pollutant concentrations lower than in 2000. The differences in VOC emissions and meteorology lead to differences in chemical aging of the pollutants; this may explain the observed differences in volume-based growth measurements in 2000 and 2006. During TexAQS-2006, more than 60% of the aerosol mass in the oxidized, aged ship channel plumes was OA, and the rest mostly ammonium sulfate. This is consistent with the conjecture of *Brock et al.* [2003] that the aerosol growth in the ship channel plumes measured in 2000 was primarily due to SOA formation.

[52] Particle composition measurements during TexAQS-2006 are also used to examine the possibility of acid catalyzed SOA formation. Because SO_2 and particle volume data downwind of the Houston ship channel were highly correlated in 2000, acid-catalyzed SOA formation was speculated to have contributed to the observed growth [*Brock et al.*, 2003]. On 26 September 2006, no evidence of fresh, small acidic sulfate particles was found even in SO_2-rich regions of the ship channel plume, and the average molar ratio of NH_4^+/SO_4^{2-} was close to 2 even for transport ages of <2 h indicating dominance of neutralized particles, yet a rapid increase in ΔOA was observed in the ship channel plume (Figure 5a). Summertime ground based measurements at the La Porte airport, Texas, ~15 km from the ship channel, also indicated that fine sulfate particles in this region are often fully neutralized [*Pavlovic et al.*, 2006]. Since the average molar ratio of NH_4^+/SO_4^{2-} in the ship channel plumes for all the flights discussed here is in the range of ~1.4–2, and since a strong increase in ΔOA is observed even in the presence of neutralized sulfate particles, consistent with other observations downwind of SO_2 sources [*Peltier et al.*, 2007; *Zhang et al.*, 2007b], we conclude that acid-catalyzed SOA formation plays at most a minor role in the observed growth of particles downwind of the industrial centers along the Houston ship channel.

8. Conclusions

[53] Measurements of OA and CO in urban plumes around Houston and Dallas/Fort Worth, Texas, and downwind of the Houston ship channel during TexAQS-2006 are reported here. Formation of SOA in the urban plumes of Houston and Dallas/Fort Worth was similar to that determined from measurements made downwind of urban areas in the NE United States. The ratio of ΔOA/ΔCO in isolated ship channel plumes on 26 September exceeded that in the Houston and Dallas urban plumes by a factor of 1.5–7, partly because of higher mixing ratios of VOCs with high aerosol formation potential in the industrial plumes. The higher production of SOA in the ship channel was not due to acid-catalyzed SOA formation.

[54] Box model simulations of SOA formation in the plumes, using recent results from laboratory studies that account for the dependence of SOA formation yield on NO_x and absorbing mass, predict OA that results in ΔOA/ΔCO values within a factor of 2 of the measurements. Accounting for SOA formation from benzene and MACR-MVK as well as the absorbing mass- and NO_x-dependent SOA yields reduce the model-measurement discrepancy compared to previous studies. On the basis of the observed improvement between the modeling results presented here and previous studies (factor of 2 here versus 3–30, for similarly aged plumes), it is of interest to apply such modeling efforts to other data sets where plumes with longer photochemical age were sampled in order to assess the ability of such models to predict SOA mass on a regional scale. The tight correlation of OA versus CO, independent of BVOC influence, indicate that anthropogenic pollution was the main contributor to SOA formation in Houston area.

[55] **Acknowledgments.** We thank the WP-3D operation crew for their efforts and support during the project, K. Aikin as the project data manager, M. Trainer for his flight planning efforts during TexAQS-2006, G. Frost and M. Trainer for discussions regarding HO_x calculations, and W. Angevine for discussions regarding the wind profiler data set. We also appreciate the constructive comments of the reviewers, which helped strengthen the manuscript. R.B. and P.F.D. acknowledge a CIRES postdoctoral visiting fellowship and an EPA STAR graduate fellowship (FP-91650801), respectively. B.E. acknowledges support from the Office of Science (BER), U.S. Department of Energy, grant DE-FG02-08ER64539.

References

Alfarra, M. R., et al. (2004), Characterization of urban and rural organic particulate in the Lower Fraser Valley using two Aerodyne Aerosol Mass Spectrometers, *Atmos. Environ.*, *38*, 5745–5758, doi:10.1016/j.atmosenv.2004.01.054.

Allan, J. D., et al. (2004), A generalized method for the extraction of chemically resolved mass spectra from Aerodyne aerosol mass spectrometer data, *J. Aerosol Sci.*, *35*(7), 909–922, doi:10.1016/j.jaerosci.2004.02.007.

Bahreini, R., E. J. Dunlea, B. M. Matthew, C. Simons, K. S. Docherty, P. F. DeCarlo, J. L. Jimenez, C. A. Brock, and A. M. Middlebrook (2008), Design and operation of a pressure-controlled inlet for airborne sampling

with an aerodynamic aerosol lens, *Aerosol Sci. Technol.*, *42*(6), 465–471, doi:10.1080/02786820802178514.

Brock, C. A., et al. (2003), Particle growth in urban and industrial plumes in Texas, *J. Geophys. Res.*, *108*(D3), 4111, doi:10.1029/2002JD002746.

Brock, C. A., et al. (2008), Sources of particulate matter in the northeastern United States in summer: 2. Evolution of chemical and microphysical properties, *J. Geophys. Res.*, *113*, D08302, doi:10.1029/2007JD009241.

Carlton, A. G., B. J. Turpin, K. E. Altieri, S. Seitzinger, A. Reff, H.-J. Lim, and B. Ervens (2007), Atmospheric oxalic acid and SOA production from glyoxal: Results of aqueous photooxidation experiments, *Atmos. Environ.*, *41*, 7588–7602, doi:10.1016/j.atmosenv.2007.05.035.

Carter, W. P. L., and R. Atkinson (1996), Development and evaluation of a detailed mechanism for the atmospheric reactions of isoprene and NO_x, *Int. J. Chem. Kinet.*, *28*(7), 497–530, doi:10.1002/(SICI)1097-4601(1996)28:7<497::AID-KIN4>3.0.CO;2-Q.

Chung, S. H., and J. H. Seinfeld (2002), Global distribution and climate forcing of carbonaceous aerosols, *J. Geophys. Res.*, *107*(D19), 4407, doi:10.1029/2001JD001397.

DeCarlo, P. F., J. G. Slowik, D. R. Worsnop, P. Davidovits, and J. L. Jimenez (2004), Particle morphology and density characterization by combined mobility and aerodynamic measurements. Part 1: Theory, *Aerosol Sci. Technol.*, *38*, 1185–1205, doi:10.1080/027868290903907.

DeCarlo, P. F., et al. (2006), Field-deployable, high-resolution, time-of-flight aerosol mass spectrometer, *Anal. Chem.*, *78*(24), 8281–8289, doi:10.1021/ac061249n.

DeCarlo, P. F., E. J. Dunlea, J. R. Kimmel, A. C. Aiken, and J. L. Jimenez (2008), Fast airborne aerosol size and chemistry measurements with the high resolution aerosol mass spectrometer during the Milagro- Mex Field Campaign, *Atmos. Chem. Phys.*, *8*, 4027–4048.

de Gouw, J. A., and C. Warneke (2007), Measurements of volatile organic compounds in the Earth's atmosphere using proton-transfer-reaction mass spectrometry, *Mass Spectrom. Rev.*, *26*, 223–257, doi:10.1002/mas.20119.

de Gouw, J. A., et al. (2005), Budget of organic carbon in a polluted atmosphere: Results from the New England Air Quality Study in 2002, *J. Geophys. Res.*, *110*, D16305, doi:10.1029/2004JD005623.

de Gouw, J. A., et al. (2008), Sources of particulate matter in the northeastern United States in summer: 1. Direct emissions and secondary formation of organic matter in urban plumes, *J. Geophys. Res.*, *113*, D08301, doi:10.1029/2007JD009243.

Drewnick, F., J. J. Schwab, J. T. Jayne, M. Canagaratna, D. R. Worsnop, and K. L. Demerjian (2004), Measurements of ambient aerosol composition during PMTACS-NY 2001 using an aerosol mass spectrometer. Part I: Mass concentrations, *Aerosol Sci. Technol.*, *38*, suppl. 1, 92–103, doi:10.1080/02786820390229507.

Drewnick, F., S. S. Hings, P. DeCarlo, J. T. Jayne, M. Gonin, K. Fuhrer, S. Weimer, J. L. Jimenez, K. L. D. S. Borrmann, and D. R. Worsnop (2005), A new time-of-flight aerosol mass spectrometer (TOF-AMS)—Instrument description and first field deployment, *Aerosol Sci. Technol.*, *39*(7), 637–658, doi:10.1080/02786820500182040.

Dunlea, E. J., et al. (2008), Evolution of Asian aerosols during transpacific transport in INTEX-B, *Atmos. Chem. Phys. Discuss.*, *8*, 15,375–15,461.

Ervens, B., and S. M. Kreidenweis (2007), SOA formation by biogenic and carbonyl compounds: Data evaluation and application, *Environ. Sci. Technol.*, *41*(11), 3904–3910, doi:10.1021/es061946x.

Ervens, B., A. G. Carlton, B. J. Turpin, K. E. Altieri, S. M. Kreidenweis, and G. Feingold (2008), Secondary organic aerosol yields from cloud-processing of isoprene oxidation products, *Geophys. Res. Lett.*, *35*, L02816, doi:10.1029/2007GL031828.

Fiore, A. M., D. J. Jacob, J. A. Logan, and J. H. Yin (1998), Long-term trends in ground level ozone over the contiguous United States, 1980–1995, *J. Geophys. Res.*, *103*(D1), 1471–1480, doi:10.1029/97JD03036.

Geron, C., R. Rasmussen, R. R. Arnts, and A. Guenther (2000), A review and synthesis of monoterpene speciation from forests in the United States, *Atmos. Environ.*, *34*(11), 1761–1781, doi:10.1016/S1352-2310(99)00364-7.

Grieshop, A. P., N. M. Donahue, and A. L. Robinson (2007), Is the gas-particle partitioning in alpha-pinene secondary organic aerosol reversible?, *Geophys. Res. Lett.*, *34*, L14810, doi:10.1029/2007GL029987.

Griffin, R. J., I. D. R. Cocker, R. C. Flagan, and J. H. Seinfeld (1999), Organic aerosol formation from the oxidation of biogenic hydrocarbons, *J. Geophys. Res.*, *104*(D3), 3555–3567, doi:10.1029/1998JD100049.

Griffin, R. J., J. Chen, K. Carmody, S. Vutukuru, and D. Dabdub (2007), Contribution of gas phase oxidation of volatile organic compounds to atmospheric carbon monoxide levels in two areas of the United States, *J. Geophys. Res.*, *112*, D10S17, doi:10.1029/2006JD007602.

Heald, C. L., D. J. Jacob, R. J. Park, L. M. Russell, B. J. Huebert, J. H. Seinfeld, H. Liao, and R. J. Weber (2005), A large organic aerosol source in the free troposphere missing from current models, *Geophys. Res. Lett.*, *32*, L18809, doi:10.1029/2005GL023831.

Hennigan, C. J., M. H. Bergin, J. E. Dibb, and R. J. Weber (2008), Enhanced secondary organic aerosol formation due to water uptake by fine particles, *Geophys. Res. Lett.*, *35*, L18801, doi:10.1029/2008GL035046.

Henze, D. K., and J. H. Seinfeld (2006), Global secondary organic aerosol from isoprene oxidation, *Geophys. Res. Lett.*, *33*, L09812, doi:10.1029/2006GL025976.

Henze, D. K., J. H. Seinfeld, N. L. Ng, J. H. Kroll, T.-M. Fu, D. J. Jacob, and C. L. Heald (2008), Global modeling of secondary organic aerosol formation from aromatic hydrocarbons: High- vs. low- yield pathways, *Atmos. Chem. Phys.*, *8*, 2405–2420.

Holloway, J. S., R. O. Jakoubek, D. D. Parrish, C. Gerbig, A. Volz-Thomas, S. Schmitgen, A. Fried, B. Wert, B. Henry, and J. R. Drummond (2000), Airborne intercomparison of vacuum ultraviolet fluorescence and tunable diode laser absorption measurements of tropospheric carbon monoxide, *J. Geophys. Res.*, *105*(D19), 24,251–24,261, doi:10.1029/2000JD900237.

Hudman, R. C., L. T. Murray, D. J. Jacob, D. B. Millet, S. Turgwety, S. Wu, D. R. Blake, A. H. Goldstein, J. Holloway, and G. W. Sachse (2008), Biogenic versus anthropogenic sources of CO in the United States, *Geophys. Res. Lett.*, *35*, L04801, doi:10.1029/2007GL032393.

Johnson, D., S. R. Utembe, M. J. Jenkin, R. G. Derwent, G. D. Hayman, M. R. Alfarra, H. Coe, and G. McFiggans (2006), Simulating regional scale secondary organic aerosol formation during the TORCH 2003 campaign in the southern UK, *Atmos. Chem. Phys.*, *6*, 403–418.

Kleinman, L. I., et al. (2008), The time evolution of aerosol composition over the Mexico City plateau, *Atmos. Chem. Phys.*, *8*, 1559–1575.

Kroll, J. H., N. L. Ng, S. M. Murphy, R. C. Flagan, and J. H. Seinfeld (2005), Secondary organic aerosol formation from isoprene photooxidation under high-NO_x conditions, *Geophys. Res. Lett.*, *32*, L18808, doi:10.1029/2005GL023637.

Kroll, J. H., N. L. Ng, S. M. Murphy, R. C. Flagan, and J. H. Seinfeld (2006), Secondary organic aerosol formation from isoprene photooxidation, *Environ. Sci. Technol.*, *40*(6), 1869–1877, doi:10.1021/es0524301.

Lemire, K. R., D. T. Allen, G. A. Klouda, and C. W. Lewis (2002), Fine particulate matter source attribution for southeast Texas using $^{14}C/^{13}C$ ratios, *J. Geophys. Res.*, *107*(D22), 4613, doi:10.1029/2002JD002339.

Lewis, C. W., and D. C. Stiles (2006), Radiocarbon content of PM2.5 ambient aerosol in Tampa, FL, *Aerosol Sci. Technol.*, *40*, 189–196, doi:10.1080/02786820500521007.

Lewis, C. W., G. A. Klouda, and W. D. Ellenson (2004), Radiocarbon measurement of the biogenic contribution to summertime PM-2.5 ambient aerosol in Nashville, TN, *Atmos. Environ.*, *38*, 6053–6061, doi:10.1016/j.atmosenv.2004.06.011.

Lim, Y. B., and P. J. Ziemann (2005), Products and mechanism of secondary organic aerosol formation from reactions of n-alkanes with OH radicals in the presence of NO_x, *Environ. Sci. Technol.*, *39*, 9229–9236, doi:10.1021/es051447g.

Mao, J., et al. (2009), Atmospheric oxidation capacity in the summer of Houston 2006: Comparison with summer measurements in other metropolitan studies, *Atmos. Environ.*, doi:10.1016/j.atmosenv.2009.01.013, in press.

Matthew, B. M., A. M. Middlebrook, and T. B. Onasch (2008), Collection efficiencies in an Aerodyne Aerosol Mass Spectrometer as a function of particle phase for laboratory generated aerosols, *Aerosol Sci. Technol.*, *42*, 884–898, doi:10.1080/02786820802356797.

Murphy, D. M., D. J. Cziczo, K. D. Froyd, P. K. Hudson, B. M. Matthew, A. M. Middlebrook, R. E. Peltier, A. Sullivan, D. S. Thomson, and R. J. Weber (2006), Single-particle mass spectrometry of tropospheric aerosol particles, *J. Geophys. Res.*, *111*, D23S32, doi:10.1029/2006JD007340.

Neuman, J. A., et al. (2009), Relationship between photochemical ozone production and NOx oxidation in Houston, Texas, *J. Geophys. Res.*, *114*, D00F08, doi:10.1029/2008JD011688.

Ng, N. L., et al. (2007a), Effect of NO_x level on secondary organic aerosol (SOA) formation from the photooxidation of terpenes, *Atmos. Chem. Phys.*, *7*, 5159–5174.

Ng, N. L., J. H. Kroll, A. W. H. Chan, P. S. Chhabra, R. C. Flagan, and J. H. Seinfeld (2007b), Secondary organic aerosol formation from m-xylene, toluene, and benzene, *Atmos. Chem. Phys.*, *7*, 3909–3922.

Odum, J. R., T. Hoffmann, F. Bowman, D. Collins, R. C. Flagan, and J. H. Seinfeld (1996), Gas/particle partitioning and secondary organic aerosol yields, *Environ. Sci. Technol.*, *30*(8), 2580–2585, doi:10.1021/es950943+.

Odum, J. R., T. P. W. Jungkamp, R. J. Griffin, R. C. Flagan, and J. H. Seinfeld (1997), The atmospheric aerosol-forming potential of whole gasoline vapor, *Science*, *276*, 96–99, doi:10.1126/science.276.5309.96.

Ortega, J., D. Helmig, A. Guenther, P. Harley, S. Pressley, and C. Vogel (2007), Flux estimates and OH reaction potential of reactive biogenic volatile organic compounds (BVOCs) from a mixed northern hardwood forest, *Atmos. Environ.*, *41*, 5479–5495, doi:10.1016/j.atmosenv.2006.12.033.

Parrish, D. D., et al. (2009), Overview of the Second Texas Air Quality Study (TexAQS II) and the Gulf of Mexico Atmospheric Composition and Climate Study (GoMACCS), *J. Geophys. Res.*, *114*, D00F13, doi:10.1029/2009JD011842.

Pavlovic, R. T., U. Nopmongcol, Y. Kimura, and D. T. Allen (2006), Ammonia emissions, concentrations and implications for particulate matter formation in Houston, TX, *Atmos. Environ.*, *40*, suppl. 2, 538–551, doi:10.1016/j.atmosenv.2006.04.071.

Peltier, R. E., A. P. Sullivan, R. J. Weber, A. G. Wollny, J. S. Holloway, C. A. Brock, J. A. deGouw, and E. L. Atlas (2007), No evidence for acid-catalyzed secondary organic aerosol formation in power plant plumes over metropolitan Atlanta, Georgia, *Geophys. Res. Lett.*, *34*, L06801, doi:10.1029/2006GL028780.

Pierce, T., and P. S. Waldruff (1991), PC-BEIS—A personal computer version of the biogenic emissions inventory system, *J. Air Waste Manage. Assoc.*, *41*(7), 937–941.

Pierce, T., C. Geron, L. Bender, R. Dennis, G. Tonnesen, and A. Guenther (1998), Influence of increased isoprene emissions on regional ozone modeling, *J. Geophys. Res.*, *103*(D19), 25,611–25,629, doi:10.1029/98JD01804.

Presto, A. A., K. E. Huff Hartz, and N. M. Donahue (2005), Secondary organic aerosol production from terpene ozonolysis. 2. Effect of NO_x concentration, *Environ. Sci. Technol.*, *39*(18), 7046–7054, doi:10.1021/es050400s.

Qin, Y., T. Walk, R. Gary, X. Yao, and S. Elles (2007), C2–C10 non-methane hydrocarbons measured in Dallas, USA—Seasonal trends and diurnal characteristics, *Atmos. Environ.*, *41*, 6018–6032, doi:10.1016/j.atmosenv.2007.03.008.

Quinn, P. K., et al. (2006), Impacts of sources and aging on submicrometer aerosol properties in the marine boundary layer across the Gulf of Maine, *J. Geophys. Res.*, *111*, D23S36, doi:10.1029/2006JD007582.

Robinson, A. L., N. M. Donahue, M. K. Shrivastava, E. A. Weitkamp, A. M. Sage, A. P. Grieshop, T. E. Lane, J. R. Pierce, and S. N. Pandis (2007), Rethinking organic aerosols: Semivolatile emissions and photochemical aging, *Science*, *315*, 1259–1262, doi:10.1126/science.1133061.

Ryerson, T. B., et al. (1998), Emissions lifetimes and ozone formation in power plant plumes, *J. Geophys. Res.*, *103*(D17), 22,569–22,583, doi:10.1029/98JD01620.

Ryerson, T. B., L. G. Huey, K. Knapp, J. A. Neuman, D. D. Parrish, D. T. Sueper, and F. C. Fehsenfeld (1999), Design and initial characterization of an inlet for gas-phase NO_y measurements from aircraft, *J. Geophys. Res.*, *104*(D5), 5483–5492, doi:10.1029/1998JD100087.

Ryerson, T. B., E. J. Williams, and F. C. Fehsenfeld (2000), An efficient photolysis system for fast-response NO_2 measurements, *J. Geophys. Res.*, *105*(D21), 26,447–26,461, doi:10.1029/2000JD900389.

Sakulyanontvittaya, T., T. Duhl, C. Wiedinmyer, D. Helmig, S. Matsunaga, M. Potosnak, J. Milford, and A. Guenther (2008), Monoterpene and sesquiterpene emission estimates for the United States, *Environ. Sci. Technol.*, *42*(5), 1623–1629, doi:10.1021/es702274e.

Schauffler, S. M., E. L. Atlas, S. G. Donnelly, A. Andrews, S. A. Montzka, J. W. Elkins, D. F. Hurst, P. A. Romashkin, G. S. Dutton, and V. Stroud (2003), Chlorine budget and partitioning during the Stratospheric Aerosol and Gas Experiment (SAGE) III Ozone Loss and Validation Experiment (SOLVE), *J. Geophys. Res.*, *108*(D5), 4173, doi:10.1029/2001JD002040.

Schichtel, B. A., W. C. Malm, G. Bench, S. Fallon, C. E. McDade, J. C. Chow, and J. G. Watson (2008), Fossil and contemporary fine particulate carbon fractions at 12 rural and urban sites in the United States, *J. Geophys. Res.*, *113*, D02311, doi:10.1029/2007JD008605.

Schwarz, J. P., et al. (2008), Measurement of the mixing state, mass, and optical size of individual black carbon particles in urban and biomass burning emissions, *Geophys. Res. Lett.*, *35*, L13810, doi:10.1029/2008GL033968.

Seinfeld, J. H., and S. N. Pandis (1998), *Atmospheric Chemistry and Physics: From Air Pollution to Climate Change*, John Wiley, New York.

Shrivastava, M. K., T. E. Lane, N. M. Donahue, S. N. Pandis, and A. L. Robinson (2008), Effects of gas particle partitioning and aging of primary emission on urban and regional organic aerosol concentrations, *J. Geophys. Res.*, *113*, D18301, doi:10.1029/2007JD009735.

Song, C., R. A. Zaveri, M. L. Alexander, J. A. Thornton, S. Madronich, J. V. Ortega, A. Zelenyuk, X. Y. Yu, A. Leskin, and D. A. Maughan (2007), Effect of hydrophobic primary organic aerosols on secondary organic aerosol formation from ozonolysis of alpha-pinene, *Geophys. Res. Lett.*, *34*, L20803, doi:10.1029/2007GL030720.

Sorooshian, A., et al. (2006), Oxalic acid in clear and cloudy atmospheres: Analysis of data from International Consortium for Atmospheric Research on Transport and Transformation 2004, *J. Geophys. Res.*, *111*, D23S45, doi:10.1029/2005JD006880.

Sorooshian, A., N. L. Ng, A. W. H. Chan, G. Feingold, R. C. Flagan, and J. H. Seinfeld (2007), Particulate organic acids and overall water-soluble aerosol composition measurements from the 2006 Gulf of Mexico Atmospheric Composition and Climate Study (GoMACCS), *J. Geophys. Res.*, *112*, D13201, doi:10.1029/2007JD008537.

Stark, H., B. M. Lerner, R. Schmitt, R. Jakoubek, E. J. Williams, T. B. Ryerson, D. T. Sueper, D. D. Parrish, and F. C. Fehsenfeld (2007), Atmospheric in situ measurement of nitrate radical (NO3) and other photolysis rates using spectroradiometry and filter radiometry, *J. Geophys. Res.*, *112*, D10S04, doi:10.1029/2006JD007578.

Stohl, A., C. Forster, A. Frank, P. Seibert, and G. Wotawa (2005), Technical note: The Lagrangian particle dispersion model FLEXPART version 6.2, *Atmos. Chem. Phys.*, *5*, 2461–2474.

Sullivan, A. P., R. E. Peltier, C. A. Brock, J. A. deGouw, J. S. Holloway, C. Warneke, A. G. Wollny, and R. J. Weber (2006), Airborne measurements of carbonaceous aerosol soluble in water over northeastern United States: Method development and an investigation into water-soluble organic carbon sources, *J. Geophys. Res.*, *111*, D23S46, doi:10.1029/2006JD007072.

Volkamer, R., J. L. Jimenez, F. SanMartini, K. Dzepina, Q. Zhang, D. Salcedo, L. T. Molina, D. R. Worsnop, and M. J. Molina (2006), Secondary organic aerosol formation from anthropogenic air pollution: Rapid and higher than expected, *Geophys. Res. Lett.*, *33*, L17811, doi:10.1029/2006GL026899.

Volkamer, R., F. SanMartini, L. T. Molina, D. Salcedo, J. L. Jimenez, and M. J. Molina (2007), A missing sink for gas-phase glyoxal in Mexico City: Formation of secondary organic aerosol, *Geophys. Res. Lett.*, *34*, L19807, doi:10.1029/2007GL030752.

Volkamer, R., P. J. Ziemann, and M. J. Molina (2009), Secondary organic aerosol formation from acetylene (C_2H_2): Seed effect on SOA yields due to organic photochemistry in the aerosol aqueous phase, *Atmos. Chem. Phys.*, *8*, 14,841–14,892.

Warneke, C., et al. (2007), Determination of urban volatile organic compound emission ratios and comparison with an emissions database, *J. Geophys. Res.*, *112*, D10S47, doi:10.1029/2006JD007930.

Weber, R. J., et al. (2007), A study of secondary organic aerosol formation in the anthropogenic-influenced southeastern United States, *J. Geophys. Res.*, *112*, D13302, doi:10.1029/2007JD008408.

Weibring, P., D. Richter, J. G. Walega, and A. Fried (2007), First demonstration of a high performance difference frequency spectrometer on airborne platforms, *Opt. Express*, *15*(21), 13,476–13,495, doi:10.1364/OE.15.013476.

Wilson, J. C., B. G. Lafleur, H. Hilbert, W. R. Seebaugh, J. Fox, D. W. Gesler, C. A. Brock, B. J. Huebert, and J. Mullen (2004), Function and performance of a low turbulence inlet for sampling supermicron particles from aircraft platforms, *Aerosol Sci. Technol.*, *38*(8), 790–802, doi:10.1080/027868290500841.

Zhang, Q., C. O. Stanier, M. R. Canagaratna, J. T. Jayne, D. R. Worsnop, S. N. Pandis, and J. L. Jimenez (2004), Insights into the chemistry of new particle formation and growth events in Pittsburgh based on aerosol mass spectrometry, *Environ. Sci. Technol.*, *38*(18), 4797–4809, doi:10.1021/es035417u.

Zhang, Q., D. R. Worsnop, M. R. Canagaratna, and J. L. Jimenez (2005), Hydrocarbon-like and oxygenated organic aerosols in Pittsburgh: Insights into sources and processes of organic aerosols, *Atmos. Chem. Phys.*, *5*, 3289–3311.

Zhang, Q., et al. (2007a), Ubiquity and dominance of oxygenated species in organic aerosols in anthropogenically influenced Northern Hemisphere midlatitudes, *Geophys. Res. Lett.*, *34*, L13801, doi:10.1029/2007GL029979.

Zhang, Q., J. L. Jimenez, D. R. Worsnop, and M. Canagaratna (2007b), A case study of urban particle acidity and its influence on secondary organic aerosol, *Environ. Sci. Technol.*, *41*(9), 3213–3219, doi:10.1021/es061812j.

E. Atlas, Rosenstiel School of Marine and Atmospheric Science, University of Miami, Miami, FL 33149, USA.

R. Bahreini, J. Brioude, J. A. de Gouw, B. Ervens, F. C. Fehsenfeld, J. S. Holloway, J. L. Jimenez, J. A. Neuman, J. Peischl, H. Stark, and C. Warneke, Cooperative Institute for Research in Environmental Sciences, University of Colorado at Boulder, Boulder, CO 80309, USA. (roya.bahreini@noaa.gov)

C. A. Brock, A. M. Middlebrook, and T. B. Ryerson, Earth System Research Laboratory, NOAA, Boulder, CO 80305, USA.

P. F. DeCarlo, Paul Scherrer Institut, CH-5232 Villigen PSI, Switzerland.

A. Fried, D. Richter, J. Walega, and P. Weibring, Earth Observing Laboratory, National Center for Atmospheric Research, Boulder, CO 80307, USA.

A. G. Wollny, Max Planck Institute for Chemistry, D-55020 Mainz, Germany.